*Structural Engineering and Mechanics, Vol. 16, No. 5 (2003) 533-556*
DOI: http://dx.doi.org/10.12989/sem.2003.16.5.533


# On complex flutter and buckling analysis of a beam structure subjected to static follower force

Q. Wang†

*Department of Mechanical, Materials and Aerospace Engineering, University of Central Florida Orlando, FL 32816-2450, USA*

*(Received November 8, 2002, Accepted July 28, 2003)*

**Abstract.** The flutter and buckling analysis of a beam structure subjected to a static follower force is completely studied in the paper. The beam is fixed in the transverse direction and constrained by a rotational spring at one end, and by a translational spring and a rotational spring at the other end. The co-existence of flutter and buckling in this beam due to the presence of the follower force is an interesting and important phenomenon. The results from this theoretical analysis will be useful for the stability design of structures in engineering applications, such as the potential of flutter control of aircrafts by smart materials. The transition-curve surface for differentiating the two distinct instability regions of the beam is first obtained with respect to the variations of the stiffness of the springs at the two ends. Second, the capacity of the follower force is derived for flutter and buckling of the beam as a function of the stiffness of the springs by observing the variation of the first two frequencies obtained from dynamic analysis of the beam. The research in the paper may be used as a benchmark for the flutter and buckling analysis of beams.

**Key words:** flutter analysis; buckling analysis; stability of structures; linearized approach, structural analysis; Euler-Bernoulli beam; follower force.

## 1. Introduction

The instability analysis of structures under dynamic compression has been completely discussed by Bolotin in his monograph (1964). The flutter and buckling analysis of beams under static follower and/or non-follower force has attracted more attention and interest among mechanics community. The static buckling is one of the instability behaviours of bending beams. It is referred to the change of the equilibrium state of a beam from one configuration to another one at a static critical compression. On the other hand, the static flutter refers to the phenomenon that the amplitude of vibration of a beam due to an initial disturbance grows without limit due to the static compression subjected to the beam. In the monograph by Timoshenko and Gere (1961), the mathematical solutions for the buckling capacity of a beam with different boundary conditions subjected to compression were listed. In addition, the flutter analysis of a cantilever beam was also briefly discussed in the monograph. In the following sections, all discussions about the buckling and flutter will be conducted only under the condition that the structure is subjected to static compression. Therefore, we omit "static" hereinafter for the sake of clarity.

† Associate Professor

Buckling is usually due to both non-follower compression and follower compression subjected to the beams. However, flutter may only occur to beams subjected to follower compression. A non-follower force is usually referred as an axial force with its direction remaining constant during the deformation of the structure. A follower force, on the other hand, is different from the non-follower force mentioned above in the sense that the direction of this type of force remains tangent to the deflection curve at the top of the column.

The classical problem about the stability of a beam fully fixed at one end and subjected at the other to a tangential compressive, or follower force, was first attempted by Pfluger (1950) and Feodosév (1953). They showed that there are no forms of equilibrium close to the undeformed form, hence, there was no buckling solution for this problem. They concluded that the beam with follower force is stable all the time. This erroneous conclusion was debated by Beck (1952) who first solved this instability problem of the beam mentioned above in view of dynamic analysis. Hence the flutter of beams had been received considerable interests since then. And the problem of the flutter of the cantilever beam under follower force is usually referred to the problem of Beck's column.

The critical follower force for the flutter of a cantilever beam was calculated as well by Deineko, Leonov (1955), and Bolotin (1963). In the paper by Deineko and Leonov (1955), an approximation was also given for a beam with two concentrated masses attached. A more accurate critical load was obtained by Jankovic (1993). Carr and Malhardeen (1979) and Leipholz (1983) have proved that Beck's column is stable when the follower force is less than the critical value obtained by Beck (1952). Further development on the analysis of Beck's column has been carried out since the fifties and sixties. Hauger and Vetter (1976) looked into the influence of elastic foundation of Winkler type on the stability of Beck's column. The influence of a pulsating force was investigated by Atanackovic and Cveticanin (1994). The optimal shape of Beck's column was given by Hanaoka and Washizu (1979). Mathsuda *et al*. (1993) analyzed the influence of variable cross-section and shear stresses on the value of the critical force. Sugiyama and his group (1995) did a lot of excellent work on the flutter analysis of structures. One experimental study is on the flutter of cantilevered columns under rocked thrust, which is one of the best lab demonstrations of follower compression on beam structures.

A complex and interesting study on the stability analysis of a general beam structure is the co-existence of flutter and buckling due to a follower compression. One of the examples is the instability of a beam subjected to a follower force with one end fixed, but restrained by a translational spring at the other end. As indicated above, if the stiffness of the spring is zero, the beam may fail by flutter from the solution for Beck's column. On the other hand, if the stiffness of the spring is infinite, the well-known result for the analysis of a propped cantilever beam shows that the buckling capacity of the beam is $p = \dfrac{\pi^2 EI}{(0.699L)^2} \approx 2.047\pi^2 EI/L^2$ (Bolotin 1963, Timoshenko and Gere 1961) both for follower compression and non-follower compression. Hence, it can be concluded logically that there must be a critical value of the spring stiffness below which the beam may fail by flutter and above which the beam may buckle only (Sundararajan 1974). Kounadis (1983) obtained some results on the boundary between flutter and divergence instability of a beam structure. Wang (2002) studied the possibility of the enhancement of the flutter and buckling capacity of a thin column with the same boundary condition by a piezoelectric layer. Additional excellent researches conducted on the linear flutter and buckling analysis can also be found by

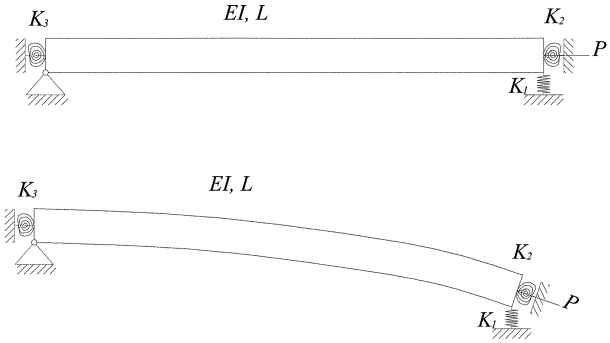


Fig. 1(a) Layout of the beam subjected to a follower force

Kounadis (1981), Bailey and Haines (1981), Kounadis and Katsikadelis (1980), and Pedersen (1977).

Actually, static buckling and flutter analysis can be categorized as linearized approach in dealing with instability analysis of undamped structures. More complex instability studies on either undamped or damped structures under dynamic loading have been conducted as well. Some fruitful results have been obtained so far by Kounadis (1991, 1998), Bolotin *et al*. (1998), Ryu and Sugiyama (2003), Langthjem and Sugiyama (2000), and Andersen and Thompsen (2002).

This paper will provide a compete study on the instability of a general undamped beam structure subjected to a static follower force. Hence, the method in the paper is strictly based on a mere undamped linearized approach. The beam under investigation is fixed in the transverse direction and constrained by a rotational spring at one end, and by a translational spring and a rotational spring at the other shown in Fig. 1(a). The flutter and buckling analysis of the beam will be fully studied analytically. The detailed analysis on the effect of spring stiffness on the possible type of the instability of the beam is conducted theoretically and numerically. The critical surface to differentiate the flutter and buckling of the beam in the co-ordinate system with respect to the stiffness of the three springs is obtained. The capacity of the follower force is also derived for different scenarios of the stiffness of the springs. The dual instability phenomenon of the beam structure due to the translational and rotational spring constraints is interesting in the field of structural stability and dynamics. One of the examples is the stability analysis of a piezoelectric layer under the induced force by piezoelectric effect which can be modelled as follower force. Besides, the results from this research may be useful for the stability design and control of structures. For example, how to control the flutter of an aircraft by smart materials is an interesting and practical problem. The research may be used as benchmark for the flutter and buckling analysis of beams.

## 2. Transition condition for flutter and buckling of the beam

The transition condition of the flutter and buckling phenomena of the beam in Fig. 1(a) will be discussed by the buckling analysis of the beam. The curved surface for differentiating flutter and buckling with respect to the stiffness of springs will be given hereinafter.

### 2.1 Derivation of the curved surface with respect to $\bar{k}_1$-$\bar{k}_2$-$\bar{k}_3$

Consider a beam subjected to a follower force $P$ as shown in Fig. 1(a). The beam is with length $L$, cross area $A$, flexural stiffness $EI$, and the mass density per unit length $\rho$. The beam is fixed transversely and constrained by a rotational spring with stiffness $k_3$ at the left end. At the right end, the beam is constrained by a translational spring with stiffness $k_1$ and a rotational spring with stiffness $k_2$. Let $x$ denote the co-ordinate along the length of the beam with its origin at the left end of the beam. The positive direction of the deflection of the beam, $u(x, t)$, is defined downward.

The shear deformation and rotary inertia effect in the structure are omitted in the model of this thin and long beam, thus the governing equation based on the Euler-Bernoulli beam model for the buckling analysis is given in a linear form,

$$EI\frac{d^4u(x)}{dx^4} + P\frac{d^2u(x)}{dx^2} = 0 \tag{1}$$

whose general solution can be expressed as

$$u(x) = A_1\cos\lambda x + A_2\sin\lambda x + A_3x/L + A_4 \tag{2}$$

where $\lambda = \sqrt{\frac{P}{EI}}$.

The buckling capacities of the structure can be obtained by searching for the non-trivial solution for $A_i(i = 1, 2, 3, 4)$ when considering the boundary conditions of the beam.

The boundary conditions for the beam in Fig. 1(a) can be expressed as:

$$u(0) = 0 \tag{3}$$

$$\left.\frac{d^2u(x)}{dx^2}\right|_{x=0} - \frac{k_3}{EI}\left.\frac{du(x)}{dx}\right|_{x=0} = 0 \tag{4}$$

$$\left.\frac{d^2u(x)}{dx^2}\right|_{x=L} + \frac{k_2}{EI}\left.\frac{du(x)}{dx}\right|_{x=L} = 0 \tag{5}$$

$$\left.\frac{d^3u(x)}{dx^3}\right|_{x=L} - \frac{k_1}{EI}u(L) = 0 \tag{6}$$

By substituting Eq. (2) into the boundary conditions of Eqs. (3)-(6), the following equations governing the four coefficients $A_i(i = 1, 2, 3, 4)$ will be obtained,

$$A_4 = -A_1 \tag{7}$$

$$-\lambda^2L^2A_1 - \bar{k}_3(\lambda LA_2 + A_3) = 0 \tag{8}$$

$$-\lambda^2L^2(A_1\cos\lambda L + A_2\sin\lambda L) + \bar{k}_2\lambda L(-A_1\sin\lambda L + A_2\cos\lambda L + A_3/\lambda L) = 0 \tag{9}$$

$$\lambda^3L^3(A_1\sin\lambda L - A_2\cos\lambda L) - \bar{k}_1(A_1\cos\lambda L + A_2\sin\lambda L + A_3 + A_4) = 0 \tag{10}$$

From Eqs. (7) and (8), we have the expressions for $A_1$ and $A_4$ in terms of $A_2$ and $A_3$ as follows:

$$A_1 = -\frac{\bar{k}_3}{\lambda^2 L^2}(\lambda L A_2 + A_3) \tag{11}$$

$$A_4 = \frac{\bar{k}_3}{\lambda^2 L^2}(\lambda L A_2 + A_3) \tag{12}$$

Substituting Eqs. (11)-(12) into Eqs. (9) and (10) yields,

$$\Delta_1 A_2 + \Delta_2 A_3 = 0 \tag{13}$$

$$\Delta_3 A_2 + \Delta_4 A_3 = 0 \tag{14}$$

where

$$\Delta_1 = -\lambda^2 L^2 \sin\lambda L + \bar{k}_2 \lambda L \cos\lambda L - \frac{\bar{k}_3}{\lambda L}(-\lambda^2 L^2 \cos\lambda L - \bar{k}_2 \lambda L \sin\lambda L) \tag{15}$$

$$\Delta_2 = -\bar{k}_2 - \frac{\bar{k}_3}{\lambda L}(-\lambda^2 L^2 \cos\lambda L - \bar{k}_2 \lambda L \sin\lambda L) \tag{16}$$

$$\Delta_3 = -\lambda^3 L^3 \cos\lambda L - \bar{k}_1 \sin\lambda L - \frac{\bar{k}_3}{\lambda L}(\lambda^3 L^3 \sin\lambda L - \bar{k}_1 \cos\lambda L + \bar{k}_1) \tag{17}$$

$$\Delta_4 = -\bar{k}_1 - \frac{\bar{k}_3}{\lambda^2 L^2}(\lambda^3 L^3 \sin\lambda L - \bar{k}_1 \cos\lambda L + \bar{k}_1) \tag{18}$$

and the non-dimensional stiffness of springs $\bar{k}_1 = \frac{k_1 L^3}{EI}$, $\bar{k}_2 = \frac{k_2 L}{EI}$, and $\bar{k}_3 = \frac{k_3 L}{EI}$.

The condition for the non-trivial solutions for $A_2$ and $A_3$ requires the solution of an eigen-value problem.

$$\Delta_1 \Delta_4 - \Delta_2 \Delta_3 = 0 \tag{19}$$

From Eq. (19), the expression for $\bar{k}_2$ can be obtained explicitly,

$$\bar{k}_2 = \frac{\bar{k}_3 \cos\lambda L \Delta_3 - (\lambda L \bar{k}_3 \cos\lambda L - \lambda^2 L^2 \sin\lambda L)\Delta_4}{(\lambda L \cos\lambda L + \bar{k}_3 \sin\lambda L)\Delta_4 - \left(1 + \frac{\bar{k}_3}{\lambda L}\sin\lambda L\right)\Delta_3} \tag{20}$$

The way to determine the transition surface for the flutter and buckling of the beam is found by searching for the minimum $\bar{k}_2$ at given $\bar{k}_1$ and $\bar{k}_3$ based on the above expression. The physical meaning for the above procedure lies in the fact that the buckling will govern the type of the instability of the beam beyond the critical value of $\bar{k}_2$ at given $\bar{k}_1$ and $\bar{k}_3$, or above the curved surface in the 3-dimensional ordinate system $\bar{k}_1$-$\bar{k}_2$-$\bar{k}_3$.

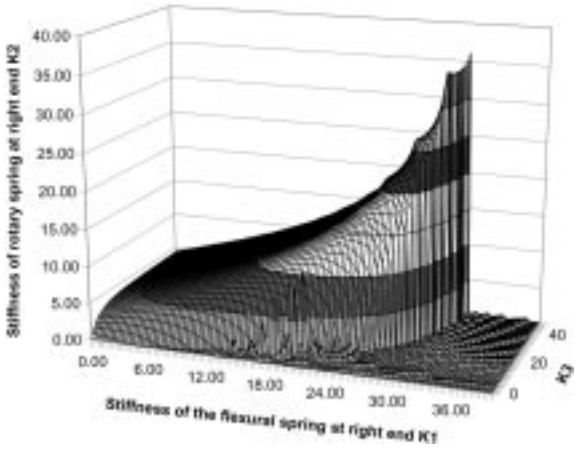


Fig. 1(b) Boundary of the flutter and buckling of the beam

The minimum $\bar{k}_2$ at given $\bar{k}_1$ and $\bar{k}_3$ is plotted in Fig. 1(b). It is observed that if the left end of the beam is pinned, i.e. $\bar{k}_3 = 0$, the beam will only show its instability in buckling form at any given spring constraint conditions.

This conclusion may also be derived from Eq. (20) when $\bar{k}_3 = 0$,

$$\bar{k}_2 = \frac{-\lambda^2 L^2 \sin\lambda L \bar{k}_1}{-\lambda L \cos\lambda L \bar{k}_1 + \lambda^3 L^3 \cos\lambda L + \bar{k}_1 \sin\lambda L} \tag{21}$$

From which the minimum $\bar{k}_2$ is zero.

Also of special interest is the case when $\bar{k}_3 = \infty$, i.e. the left end is fixed. An interesting and practical question arises as to what the critical values for $\bar{k}_1$ and $\bar{k}_2$ will be to differentiate the types of the instability of the beam. These values can, of course, be determined from the numerical calculations. However, theoretical analysis on this problem will be more attractive to the applied mechanics community.

Next, the following three problems will be conducted when $\bar{k}_3 = \infty$:

(a) the derivation of the critical value of $\bar{k}_1$ at $\bar{k}_2 = 0$;

(b) the derivation of the critical value of $\bar{k}_2$ at $\bar{k}_1 = 0$;

(c) the derivation of the transition curve $\bar{k}_1$-$\bar{k}_2$.

### *2.2 Derivation of the critical value $\bar{k}_1$ when $\bar{k}_3 = \infty$ (Sundararajan 1974)*

The determination of the critical value $\bar{k}_1$ for the transition of flutter and buckling of the beam at $\bar{k}_2 = 0$ can be obtained by using the above buckling analysis to search for the minimum $\bar{k}_1$ beyond which the buckling phenomenon may be initiated.

Eq. (19) changes to the following equation at $\bar{k}_2 = 0$ and $\bar{k}_3 = \infty$,

$$\bar{k}_1(\lambda L \cos\lambda L - \sin\lambda L) = \lambda^3 L^3 \tag{22}$$

The minimum of $\bar{k}_1$ for the existence of Eq. (22) can be determined by the following calculation of the non-dimensional variable $\lambda L$,

$$\frac{d}{d(\lambda L)}\left(\frac{\lambda^3 L^3}{\lambda L\cos\lambda L - \sin\lambda L}\right) = 0 \quad \text{when } \lambda L\cos\lambda L - \sin\lambda L > 0 \tag{23}$$

$$\text{i.e. } (\lambda L)^2\sin\lambda L + 3\lambda L\cos\lambda L - 3\sin\lambda L = 0 \quad \text{when } \lambda L\cos\lambda L - \sin\lambda L > 0 \tag{24}$$

The final solution for the minimum $\bar{k}_1$ in Eq. (24) is $\bar{k}_1 = 34.8$.

This solution reveals a very interesting conclusion that when the spring stiffness is less than the critical value, the instability of the beam is of flutter type. Otherwise, the beam may fail by buckling only.

### *2.3 Derivation of the critical value $\bar{k}_2$ at $\bar{k}_1 = 0$*

The determination of the critical value $\bar{k}_2$ for the transition of flutter and buckling of the beam at $\bar{k}_1 = 0$ can be derived in a similar way.

At $\bar{k}_1 = 0$ and $\bar{k}_3 = \infty$, (19) changes to

$$\bar{k}_2 = -\frac{\lambda L}{\sin\lambda L} \tag{25}$$

Similarly, the minimum of $\bar{k}_2$ for the existence of Eq. (25) can be determined by the following calculation of $\lambda L$,

$$\frac{d}{d(\lambda L)}\left(\frac{\lambda L}{\sin\lambda L}\right) = 0 \quad \text{when } \sin\lambda L < 0 \tag{26}$$

which leads to the value $\bar{k}_2 \approx 4.6$ after which the instability of the beam is in its buckling form.

### *2.4 Derivation of the $\bar{k}_1 - \bar{k}_2$ transition curve*

Next, the $\bar{k}_1 - \bar{k}_2$ transition curve for flutter and buckling of the beam at $\bar{k}_3 = \infty$ can be obtained from the buckling result of the beam shown in Eq. (19) as follows.

$$\bar{k}_2 = -\frac{\lambda L(-\lambda^3 L^3 + \bar{k}_1\lambda L\cos\lambda L - \bar{k}_1\sin\lambda L)}{\bar{k}_1\lambda L\sin\lambda L - \lambda^3 L^3\sin\lambda L + 2\bar{k}_1(\cos\lambda L - 1)} \tag{27}$$

The procedure is to search for the minimum $\bar{k}_2$ which will satisfy the equality of Eq. (27) among all the possible solutions of $\lambda L$ for any given value of $\bar{k}_1$.

The minimum of $\bar{k}_2$ at a given $\bar{k}_1$ can be determined by a similar calculation of $\lambda L$.

Fig. 1(c) plots the transition curve of $\bar{k}_1 - \bar{k}_2$. It is noted from this plot that the concave curve starts at $\bar{k}_1 = 0, \bar{k}_2 \approx 4.6$ and ends at $\bar{k}_1 \approx 34.8, \bar{k}_2 \approx 47.6$. This observation coincides with the results from Sections 2.2 and 2.3. Only under the curve and within the vertical straight line $\bar{k}_1 = 34.8$, can flutter occur on the beam. Otherwise, the instability of the beam may only occur in the form of buckling.

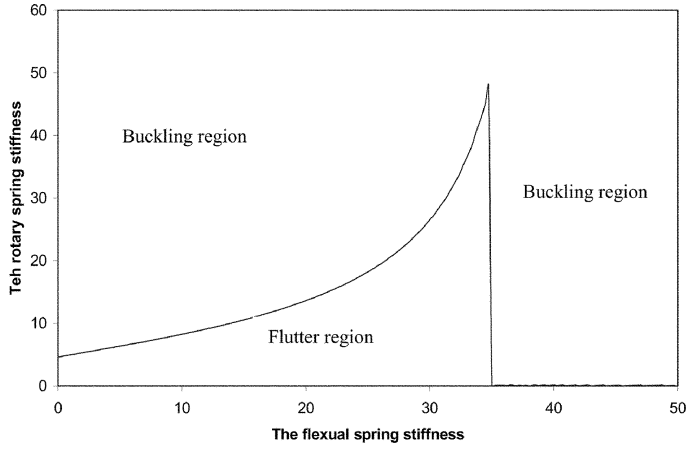


Fig. 1(c) The transition curve of flutter and buckling of the beam at $k_3 = \infty$

The magnitudes of the follower force for flutter and buckling analysis of the beam are of importance in the design of beam structures after the transition surface is obtained, and will be conducted below.

## 3. The capacities of the follower force for the flutter and buckling of the beam

The derivation of the capacities of the follower force will be conducted through the vibration analysis of the beam. The form of the instability of the beam may be derived by observation from the variation of the first two frequencies of the beam which will be illustrated below.

### *3.1 Instability analysis of the beam*

The governing equation based on the Euler-Bernoulli beam model for the linear flutter analysis of the beam shown in Fig. 1(a) is given by

$$EI\frac{\partial^4 u}{\partial x^4} + P\frac{\partial^2 u}{\partial x^2} + \rho A\frac{\partial^2 u}{\partial t^2} = 0 \tag{28}$$

The general solution of Eq. (28) is written as

$$u(x,t) = U(x)e^{i\omega t} \tag{29}$$

where $\omega$ is the circular frequency of the beam and $U(x)$ is the admissible shape for the beam vibrating at frequency $\omega$.

Substituting Eq. (29) into Eq. (28) yields the governing equation for the function $U(x)$,

$$EI\frac{d^4 U}{dx^4} + P\frac{d^2 U}{dx^2} - \rho A\omega^2 U = 0 \tag{30}$$

whose general solution is found to be,

$$U(x) = B_1\cos\beta_1 x + B_2\sin\beta_1 x + B_3\cosh\beta_2 x + B_4\sinh\beta_2 x \tag{31}$$

where

$$\beta_1 = \sqrt{(\mu^2 + \lambda^4/4)^{1/2} + \lambda^2/2} \tag{32}$$

$$\beta_2 = \sqrt{(\mu^2 + \lambda^4/4)^{1/2} - \lambda^2/2} \tag{33}$$

$$\lambda^2 = \frac{P}{EI} \tag{34}$$

$$\mu^2 = \frac{\rho A\omega^2}{EI} \tag{35}$$

The flutter capacities of the structure can be obtained by determining the condition of the non-trivial solution for $B_i (i = 1, 2, 3, 4)$. Substituting the expression of $U(x)$ from Eq. (31) into the boundary condition in Eqs. (3)-(6) yields the following four equations respectively,

$$B_3 = -B_1 \tag{36}$$

$$-\beta_1^2 L^2 B_1 + \beta_2^2 L^2 B_3 - \bar{k}_3(\beta_1 L B_2 + \beta_2 L B_4) = 0 \tag{37}$$

$$\begin{aligned} &-\beta_1^2 L^2(B_1\cos\beta_1 L + B_2\sin\beta_1 L) + \beta_2^2 L^2(B_3\cosh\beta_2 L + B_4\sinh\beta_2 L) \\ &+ \bar{k}_2(-B_1\beta_1 L\sin\beta_1 L + B_2\beta_1\cos\beta_1 L + B_3\beta_2 L\sinh\beta_2 L + B_4\beta_2 L\cosh\beta_2 L) = 0 \end{aligned} \tag{38}$$

$$\begin{aligned} &\beta_1^3 L^3(B_1\sin\beta_1 L - B_2\cos\beta_1 L) + \beta_2^3 L^3(B_3\sinh\beta_2 L + B_4\cosh\beta_2 L) - \\ &\bar{k}_1(B_1\cos\beta_1 L + B_2\sin\beta_1 L + B_3\cosh\beta_2 L + B_4\sinh\beta_2 L) = 0 \end{aligned} \tag{39}$$

From Eqs. (36)-(37), $B_1$ and $B_3$ can be expressed in terms of $B_2$ and $B_4$ as follows,

$$B_1 = -\frac{\bar{k}_3}{\beta_1^2 L^2 + \beta_2^2 L^2}(\beta_1 L B_2 + \beta_2 L B_3) \tag{40}$$

$$B_3 = \frac{\bar{k}_3}{\beta_1^2 L^2 + \beta_2^2 L^2}(\beta_1 L B_2 + \beta_2 L B_3) \tag{41}$$

Substituting Eqs. (40)-(41) into Eqs. (38)-(39) yields,

$$\Delta_5 B_2 + \Delta_6 B_3 = 0 \tag{42}$$

$$\Delta_7 B_2 + \Delta_8 B_3 = 0 \tag{43}$$

where

$$\Delta_5 = -\beta_1^2 L^2 \sin\beta_1 L + \bar{k}_2 \beta_1 L \cos\beta_1 L - \frac{\bar{k}_3 \beta_1 L}{\beta_1^2 L^2 + \beta_2^2 L^2}(-\beta_1^2 L^2 \cos\beta_1 L - \bar{k}_2 \beta_1 L \sin\beta_1 L) + \frac{\bar{k}_3 \beta_1 L}{\beta_1^2 L^2 + \beta_2^2 L^2}(\beta_2^2 L^2 \cosh\beta_2 L + \bar{k}_2 \beta_2 L \sinh\beta_2 L) \tag{44}$$

$$\Delta_6 = \beta_2^2 L^2 \sinh\beta_2 L + \bar{k}_2 \beta_2 L \cosh\beta_2 L - \frac{\bar{k}_3 \beta_2 L}{\beta_1^2 L^2 + \beta_2^2 L^2}(-\beta_1^2 L^2 \cos\beta_1 L - \bar{k}_2 \beta_1 L \sin\beta_1 L) + \frac{\bar{k}_3 \beta_2 L}{\beta_1^2 L^2 + \beta_2^2 L^2}(\beta_2^2 L^2 \cosh\beta_2 L + \bar{k}_2 \beta_2 L \sinh\beta_1 L) \tag{45}$$

$$\Delta_7 = -\beta_1^3 L^3 \cos\beta_1 L - \bar{k}_1 \sin\beta_1 L - \frac{\bar{k}_3 \beta_1 L}{\beta_1^2 L^2 + \beta_2^2 L^2}(\beta_1^3 L^3 \sin\beta_1 L - \bar{k}_1 \sin\beta_1 L) + \frac{\bar{k}_3 \beta_1 L}{\beta_1^2 L^2 + \beta_2^2 L^2}(\beta_2^3 L^3 \sinh\beta_2 L - \bar{k}_1 \cosh\beta_2 L) \tag{46}$$

$$\Delta_8 = \beta_2^3 L^3 \cosh\beta_2 L - \bar{k}_1 \sinh\beta_2 L - \frac{\bar{k}_3 \beta_2 L}{\beta_1^2 L^2 + \beta_2^2 L^2}(\beta_1^3 L^3 \sin\beta_1 L - \bar{k}_1 \sin\beta_1 L) + \frac{\bar{k}_3 \beta_2 L}{\beta_1^2 L^2 + \beta_2^2 L^2}(\beta_2^3 L^3 \sinh\beta_2 L - \bar{k}_1 \cosh\beta_2 L) \tag{47}$$

The existence for the non-trivial solutions of $B_2$ and $B_4$ requires:

$$\Delta_5 \Delta_8 - \Delta_6 \Delta_7 = 0 \tag{48}$$

The non-dimensional frequencies $\bar{\omega}_1 = \frac{\rho A \omega_1^2 L^4}{EI}$ and $\bar{\omega}_2 = \frac{\rho A \omega_2^2 L^4}{EI}$, as well as the non-dimensional values of follower force $\bar{P} = P/P_{cr}$, where $P_{cr} = \pi^2 EI/L^2$ is Euler buckling load, are defined for the following numerical simulations.

The procedure for obtaining the flutter or buckling capacity of the beam by the follower force will be explained below. For a given follower force *P*, the first two resonant frequencies $\omega_1$ and $\omega_2$ can be obtained from Eq. (48). There is, however, a definite value of the follower force at which the values of $\omega_1$ and $\omega_2$ approach each other (Timoshenko and Gere 1961). We define the definite value of the follower force as the flutter capacity of this beam structure. On the other hand, we define the value of the follower force as the buckling capacity of the structure at which the value of $\omega_1$ reaches zero. In fact, the buckling analysis of the beam by the follower force has already been obtained theoretically in the prior section.

Table 1 The comparison of the capacities of the follower force for the flutter and buckling of the beam

| | $k_3 = \infty$ | | | | $k_3 = 0$ | |
|---|---|---|---|---|---|---|
| Spring stiffness | $\bar{k}_1=\bar{k}_2=0$ | $\bar{k}_1=\infty\,\bar{k}_2=\infty$ | $\bar{k}_1=\infty\,\bar{k}_2=0$ | $\bar{k}_1=0\,\bar{k}_2=\infty$ | $\bar{k}_1=\infty\,\bar{k}_2=0$ | $\bar{k}_1=\infty\,\bar{k}_2=\infty$ |
| Instability | Flutter | Buckling | Buckling | Buckling | Buckling | Buckling |
| $\bar{P}$ from Timoshenko and Gere (1961) | 2.035 | 4.000 | 2.050 | 1.000 | 1.000 | 2.050 |
| $\bar{P}$ from the paper | 2.040 | 3.990 | 2.070 | 0.990 | 0.990 | 2.070 |

### *3.2 Validation of the presented formulae*

Table 1 lists the flutter and buckling capacities of the beam discussed above with some standard boundary conditions. From this table, the capacities of the follower force for the beams with pinned-pinned, fixed-free, fixed-pinned, fixed-fixed, and fixed-sliding ends are derived from the current research paper and the monograph by Timoshenko and Gere (1961). This is for the purpose of validation. It can be seen that the results coincide with each other well. The differences for all the cases based on the current calculations and the solution in the monograph are within 1%.

### *3.3 Capacity of the follower force for stability analysis of the beam*

The capacities will be derived and discussed below for different scenarios. The derivation of the

Table 2 The capacities of the non-dimensional follower force $\bar{P}$ at $\bar{K}_3 = 0$

| $\bar{k}_2$ \ $\bar{k}_1$ | 2.50 | 5.00 | 7.50 | 10.00 | 12.50 | 15.00 | 17.50 | 20.00 | 22.50 | 25.00 | 27.50 | 30.00 | 32.50 | 35.00 | 37.50 | 40.00 | 42.50 | 45.00 | 47.50 | 50.00 |
|---|---|---|---|---|---|---|---|---|---|---|---|---|---|---|---|---|---|---|---|---|
| 0.00 | 0.78 | 0.90 | 0.96 | 0.96 | 0.96 | 0.96 | 0.96 | 0.96 | 0.96 | 0.96 | 0.96 | 0.96 | 0.96 | 0.96 | 1.02 | 1.02 | 1.02 | 1.02 | 1.02 | 1.02 |
| 2.00 | 0.48 | 0.72 | 0.84 | 0.96 | 1.02 | 1.08 | 1.08 | 1.14 | 1.14 | 1.14 | 1.14 | 1.20 | 1.20 | 1.20 | 1.20 | 1.20 | 1.20 | 1.20 | 1.20 | 1.26 |
| 4.00 | 0.42 | 0.66 | 0.84 | 0.96 | 1.02 | 1.08 | 1.14 | 1.20 | 1.20 | 1.26 | 1.26 | 1.26 | 1.32 | 1.32 | 1.32 | 1.32 | 1.32 | 1.38 | 1.38 | 1.38 |
| 6.00 | 0.42 | 0.66 | 0.78 | 0.96 | 1.02 | 1.14 | 1.20 | 1.26 | 1.26 | 1.32 | 1.32 | 1.38 | 1.38 | 1.38 | 1.44 | 1.44 | 1.44 | 1.44 | 1.44 | 1.44 |
| 8.00 | 0.42 | 0.60 | 0.78 | 0.96 | 1.08 | 1.14 | 1.20 | 1.26 | 1.32 | 1.38 | 1.38 | 1.44 | 1.44 | 1.44 | 1.50 | 1.50 | 1.50 | 1.50 | 1.50 | 1.50 |
| 10.00 | 0.42 | 0.60 | 0.78 | 0.96 | 1.08 | 1.14 | 1.26 | 1.32 | 1.38 | 1.38 | 1.44 | 1.44 | 1.50 | 1.50 | 1.50 | 1.56 | 1.56 | 1.56 | 1.56 | 1.56 |
| 12.00 | 0.42 | 0.60 | 0.78 | 0.96 | 1.08 | 1.20 | 1.26 | 1.32 | 1.38 | 1.44 | 1.44 | 1.50 | 1.50 | 1.56 | 1.56 | 1.56 | 1.56 | 1.62 | 1.62 | 1.62 |
| 14.00 | 0.42 | 0.60 | 0.78 | 0.96 | 1.08 | 1.20 | 1.26 | 1.32 | 1.38 | 1.44 | 1.50 | 1.50 | 1.56 | 1.56 | 1.56 | 1.62 | 1.62 | 1.62 | 1.62 | 1.62 |
| 16.00 | 0.42 | 0.60 | 0.78 | 0.96 | 1.08 | 1.20 | 1.26 | 1.32 | 1.38 | 1.44 | 1.50 | 1.56 | 1.56 | 1.56 | 1.62 | 1.62 | 1.62 | 1.62 | 1.68 | 1.68 |
| 18.00 | 0.42 | 0.60 | 0.78 | 0.96 | 1.08 | 1.20 | 1.26 | 1.38 | 1.44 | 1.50 | 1.50 | 1.56 | 1.56 | 1.62 | 1.62 | 1.62 | 1.68 | 1.68 | 1.68 | 1.68 |
| 20.00 | 0.42 | 0.60 | 0.78 | 0.96 | 1.08 | 1.20 | 1.32 | 1.38 | 1.44 | 1.50 | 1.50 | 1.56 | 1.62 | 1.62 | 1.62 | 1.68 | 1.68 | 1.68 | 1.68 | 1.68 |
| 22.00 | 0.42 | 0.60 | 0.78 | 0.96 | 1.08 | 1.20 | 1.32 | 1.38 | 1.44 | 1.50 | 1.56 | 1.56 | 1.62 | 1.62 | 1.68 | 1.68 | 1.68 | 1.68 | 1.74 | 1.74 |
| 24.00 | 0.36 | 0.60 | 0.78 | 0.96 | 1.08 | 1.20 | 1.32 | 1.38 | 1.44 | 1.50 | 1.56 | 1.56 | 1.62 | 1.62 | 1.68 | 1.68 | 1.68 | 1.74 | 1.74 | 1.74 |
| 26.00 | 0.36 | 0.60 | 0.78 | 0.96 | 1.08 | 1.20 | 1.32 | 1.38 | 1.44 | 1.50 | 1.56 | 1.62 | 1.62 | 1.68 | 1.68 | 1.68 | 1.74 | 1.74 | 1.74 | 1.74 |
| 28.00 | 0.36 | 0.60 | 0.78 | 0.96 | 1.08 | 1.20 | 1.32 | 1.38 | 1.44 | 1.50 | 1.56 | 1.62 | 1.62 | 1.68 | 1.68 | 1.68 | 1.74 | 1.74 | 1.74 | 1.74 |
| 30.00 | 0.36 | 0.60 | 0.78 | 0.96 | 1.08 | 1.20 | 1.32 | 1.38 | 1.50 | 1.50 | 1.56 | 1.62 | 1.62 | 1.68 | 1.68 | 1.74 | 1.74 | 1.74 | 1.74 | 1.74 |
| 32.00 | 0.36 | 0.60 | 0.78 | 0.96 | 1.08 | 1.20 | 1.32 | 1.38 | 1.50 | 1.56 | 1.56 | 1.62 | 1.68 | 1.68 | 1.68 | 1.74 | 1.74 | 1.74 | 1.74 | 1.80 |
| 34.00 | 0.36 | 0.60 | 0.78 | 0.96 | 1.08 | 1.20 | 1.32 | 1.44 | 1.50 | 1.56 | 1.56 | 1.62 | 1.68 | 1.68 | 1.68 | 1.74 | 1.74 | 1.74 | 1.80 | 1.80 |
| 36.00 | 0.36 | 0.60 | 0.78 | 0.96 | 1.08 | 1.20 | 1.32 | 1.44 | 1.50 | 1.56 | 1.62 | 1.62 | 1.68 | 1.68 | 1.74 | 1.74 | 1.74 | 1.74 | 1.80 | 1.80 |
| 38.00 | 0.36 | 0.60 | 0.78 | 0.96 | 1.08 | 1.20 | 1.32 | 1.44 | 1.50 | 1.56 | 1.62 | 1.62 | 1.68 | 1.68 | 1.74 | 1.74 | 1.74 | 1.80 | 1.80 | 1.80 |

following results may be used as benchmark for the stability analysis and control of beam structures.

### 3.3.1 Capacity of the follower force at $\bar{k}_3 = 0$

Table 2 lists the capacities of the non-dimensional follower force $\bar{P}$ at $\bar{k}_3 = 0$. The first row represents the variation of $\bar{k}_1$, whereas the first column stands for $\bar{k}_2$. This distribution of the capacities is also plotted in Fig. 2(a). As indicated in section 2, the form of the instability of the beam for this case is buckling solely. This conclusion can also be viewed from the smooth surface in Fig. 2(a). The variations of the first two frequencies at the pair of $\bar{k}_1$-$\bar{k}_2$ as (10,0.5) and (10,1.5) are shown in Fig. 2(b) and Fig. 2(c) respectively. The buckling loads are again clearly illustrated from the values of the non-dimensional follower force at which the first frequencies approach zero.

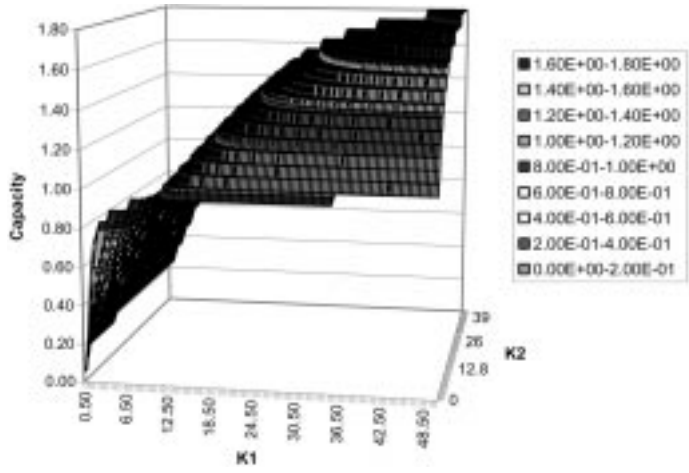


Fig. 2(a) The distribution of the capacities of the follower force at $\bar{K}_3 = 0$

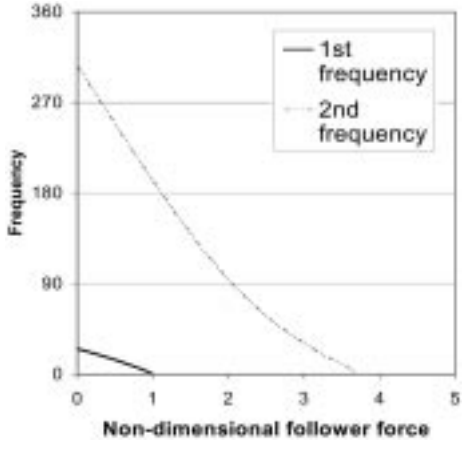


Fig. 2(b) Variation of the first two frequencies at (10,0.5)

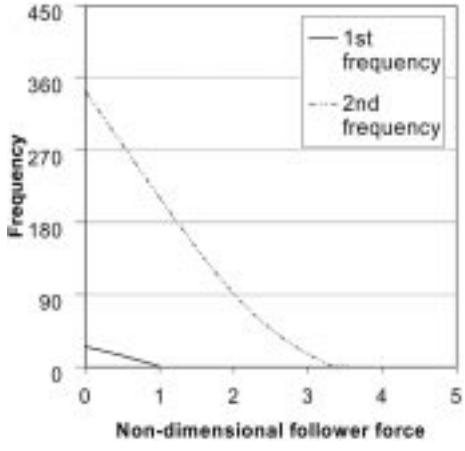


Fig. 2(c) Variation of the first two frequencies at (10,1.5)

### *3.3.2 Capacity of the follower force at $\bar{k}_3 = 2$*

Table 3 lists the capacities of the non-dimensional follower force $\bar{P}$ at $\bar{k}_3 = 2$. The distribution of the capacities is plotted in Fig. 3(a), from which the abrupt changes in the surface are found around the corner of the co-ordinate system. This portion of irregular changes represents the region in which only flutter governs the form of the instability of the beam, and hence, beyond this region the instability of the beam is in the form of buckling. This region is explicitly illustrated in Fig. 3(b). It is shown that the region covers an approximate rectangular portion between $0 < \bar{k}_1 < 8$ and

Table 3 The capacities of the non-dimensional follower force $\bar{P}$ at $\bar{K}_3 = 2$

| $\bar{k}_2$ \ $\bar{k}_1$ | 2.50 | 5.00 | 7.50 | 10.00 | 12.50 | 15.00 | 17.50 | 20.00 | 22.50 | 25.00 | 27.50 | 30.00 | 32.50 | 35.00 | 37.50 | 40.00 | 42.50 | 45.00 |
|---|---|---|---|---|---|---|---|---|---|---|---|---|---|---|---|---|---|---|
| 0.00 | 1.86 | 2.10 | 2.40 | 1.80 | 1.68 | 1.56 | 1.56 | 1.50 | 1.50 | 1.44 | 1.44 | 1.44 | 1.44 | 1.38 | 1.38 | 1.38 | 1.38 | 1.38 |
| 2.00 | 1.20 | 1.44 | 1.56 | 1.56 | 1.62 | 1.62 | 1.62 | 1.62 | 1.62 | 1.62 | 1.62 | 1.62 | 1.62 | 1.68 | 1.68 | 1.68 | 1.68 | 1.68 |
| 4.00 | 0.90 | 1.20 | 1.38 | 1.50 | 1.56 | 1.62 | 1.68 | 1.68 | 1.74 | 1.74 | 1.74 | 1.80 | 1.80 | 1.80 | 1.80 | 1.80 | 1.80 | 1.80 |
| 6.00 | 0.84 | 1.08 | 1.26 | 1.44 | 1.56 | 1.62 | 1.68 | 1.74 | 1.80 | 1.80 | 1.86 | 1.86 | 1.86 | 1.86 | 1.92 | 1.92 | 1.92 | 1.92 |
| 8.00 | 0.78 | 1.02 | 1.26 | 1.44 | 1.56 | 1.68 | 1.74 | 1.80 | 1.86 | 1.86 | 1.92 | 1.92 | 1.92 | 1.98 | 1.98 | 1.98 | 1.98 | 1.98 |
| 10.00 | 0.78 | 1.02 | 1.20 | 1.38 | 1.56 | 1.68 | 1.74 | 1.80 | 1.86 | 1.92 | 1.92 | 1.98 | 1.98 | 2.04 | 2.04 | 2.04 | 2.04 | 2.04 |
| 12.00 | 0.72 | 0.96 | 1.20 | 1.38 | 1.56 | 1.68 | 1.74 | 1.86 | 1.92 | 1.92 | 1.98 | 1.98 | 2.04 | 2.04 | 2.04 | 2.10 | 2.10 | 2.10 |
| 14.00 | 0.72 | 0.96 | 1.20 | 1.38 | 1.56 | 1.68 | 1.74 | 1.86 | 1.92 | 1.98 | 1.98 | 2.04 | 2.04 | 2.10 | 2.10 | 2.10 | 2.10 | 2.16 |
| 16.00 | 0.72 | 0.96 | 1.20 | 1.38 | 1.50 | 1.68 | 1.80 | 1.86 | 1.92 | 1.98 | 2.04 | 2.04 | 2.10 | 2.10 | 2.16 | 2.16 | 2.16 | 2.16 |
| 18.00 | 0.72 | 0.96 | 1.14 | 1.38 | 1.50 | 1.68 | 1.80 | 1.86 | 1.92 | 1.98 | 2.04 | 2.10 | 2.10 | 2.16 | 2.16 | 2.16 | 2.16 | 2.22 |
| 20.00 | 0.72 | 0.96 | 1.14 | 1.38 | 1.50 | 1.68 | 1.80 | 1.86 | 1.98 | 2.04 | 2.04 | 2.10 | 2.16 | 2.16 | 2.16 | 2.22 | 2.22 | 2.22 |
| 22.00 | 0.72 | 0.96 | 1.14 | 1.32 | 1.50 | 1.68 | 1.80 | 1.92 | 1.98 | 2.04 | 2.10 | 2.10 | 2.16 | 2.16 | 2.22 | 2.22 | 2.22 | 2.22 |
| 24.00 | 0.72 | 0.96 | 1.14 | 1.32 | 1.50 | 1.68 | 1.80 | 1.92 | 1.98 | 2.04 | 2.10 | 2.16 | 2.16 | 2.16 | 2.22 | 2.22 | 2.22 | 2.28 |
| 26.00 | 0.72 | 0.96 | 1.14 | 1.32 | 1.50 | 1.68 | 1.80 | 1.92 | 1.98 | 2.04 | 2.10 | 2.16 | 2.16 | 2.22 | 2.22 | 2.22 | 2.28 | 2.28 |
| 28.00 | 0.72 | 0.96 | 1.14 | 1.32 | 1.50 | 1.68 | 1.80 | 1.92 | 1.98 | 2.04 | 2.10 | 2.16 | 2.16 | 2.22 | 2.22 | 2.28 | 2.28 | 2.28 |
| 30.00 | 0.72 | 0.96 | 1.14 | 1.32 | 1.50 | 1.68 | 1.80 | 1.92 | 1.98 | 2.10 | 2.10 | 2.16 | 2.22 | 2.22 | 2.22 | 2.28 | 2.28 | 2.28 |
| 32.00 | 0.72 | 0.90 | 1.14 | 1.32 | 1.50 | 1.68 | 1.80 | 1.92 | 2.04 | 2.10 | 2.16 | 2.16 | 2.22 | 2.22 | 2.28 | 2.28 | 2.28 | 2.28 |
| 34.00 | 0.72 | 0.90 | 1.14 | 1.32 | 1.50 | 1.68 | 1.80 | 1.92 | 2.04 | 2.10 | 2.16 | 2.16 | 2.22 | 2.22 | 2.28 | 2.28 | 2.28 | 2.28 |
| 36.00 | 0.72 | 0.90 | 1.14 | 1.32 | 1.50 | 1.68 | 1.80 | 1.92 | 2.04 | 2.10 | 2.16 | 2.22 | 2.22 | 2.28 | 2.28 | 2.28 | 2.28 | 2.34 |
| 38.00 | 0.72 | 0.90 | 1.14 | 1.32 | 1.50 | 1.68 | 1.80 | 1.92 | 2.04 | 2.10 | 2.16 | 2.22 | 2.22 | 2.28 | 2.28 | 2.28 | 2.34 | 2.34 |

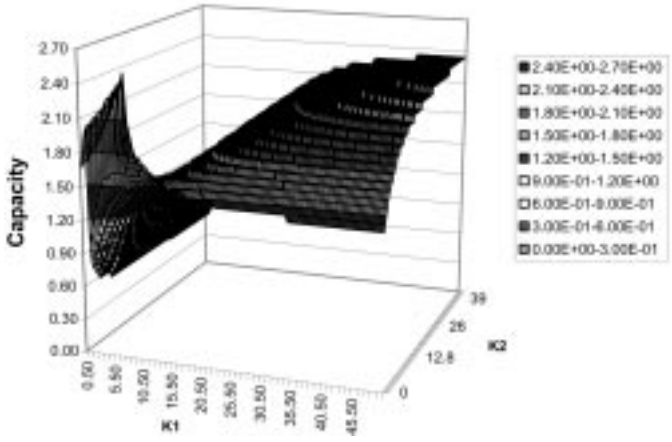


Fig. 3(a) The distribution of the capacities of the follower force at $\bar{K}_3 = 2$

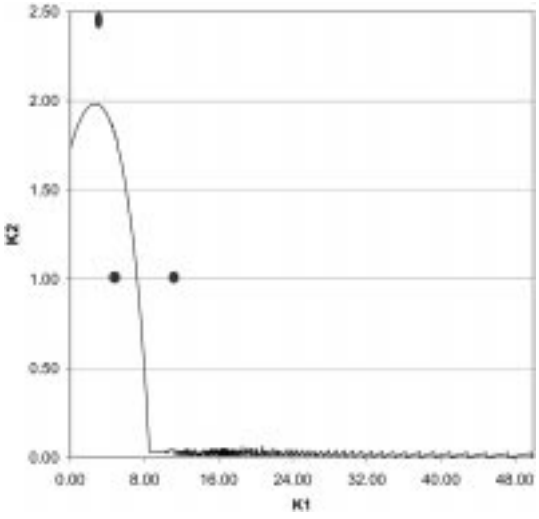


Fig. 3(b) The transition curve of the flutter and buckling instability at $\overline{K}_3 = 2$

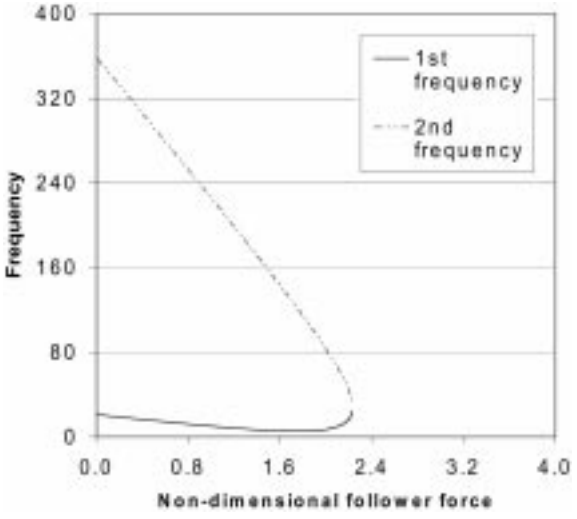


Fig. 3(c) Variation of the first two frequencies at (5,1)

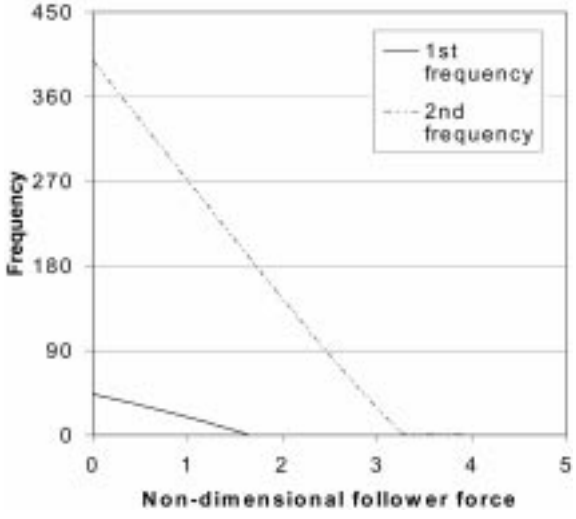


Fig. 3(d) Variation of the first two frequencies at (15,1)

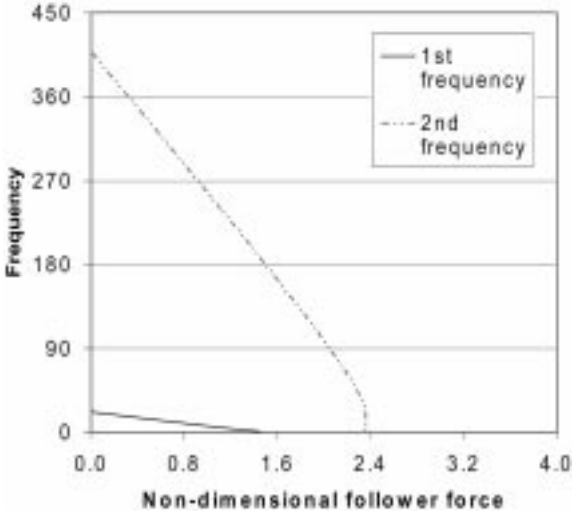


Fig. 3(e) Variation of the first two frequencies at (5, 2.5)

$0 < \overline{k}_2 < 2$. Therefore, in Table 3, the shaded parts represent the capacities of the follower force for flutter of the beam. To further illustrate the above declarations, the variations of the first two frequencies for three pairs of $\overline{k}_1$-$\overline{k}_2$, i.e. (5,1), (15,1), and (5,2.5) dotted in Fig. 3(b), are plotted in Figs. 3(c)-(e). In Fig. 3(c), the first two frequencies coalesce around $\overline{P} \approx 2.23$, which shows that at this point the beam fails only by flutter. On the other hand, in Figs. 3(d) and 3(e), the first frequencies approach zero first, which indicates that the buckling is the form of the instability at the two pairs of the $\overline{k}_1$-$\overline{k}_2$. The capacities for the two cases are around $\overline{P} = 1.61$ and $\overline{P} = 1.40$ read from the figures.

### *3.3.3 Capacity of the follower force at $\bar{k}_3 = 5$*

Table 4 lists the capacities of the non-dimensional follower force $\bar{P}$ at $\bar{k}_3 = 5$. The distribution of the capacities is similarly plotted in Fig. 4(a). The abrupt changes in the surface are investigated as well in the figure. The transition curve for differentiating the two forms of the instability of the beam is shown in Fig. 4(b) in $\bar{k}_1$-$\bar{k}_2$ co-ordinate system. Under this curve the instability is in the

Table 4 The capacities of the non-dimensional follower force $\bar{P}$ at $\bar{K}_3 = 5$

| $\bar{k}_2$ \ $\bar{k}_1$ | 2.50 | 5.00 | 7.50 | 10.00 | 12.50 | 15.00 | 17.50 | 20.00 | 22.50 | 25.00 | 27.50 | 30.00 | 32.50 | 35.00 | 37.50 | 40.00 | 42.50 | 45.00 |
|---|---|---|---|---|---|---|---|---|---|---|---|---|---|---|---|---|---|---|
| 0.00 | 1.86 | 1.98 | 2.16 | 2.34 | 2.58 | 2.82 | 2.34 | 2.16 | 2.04 | 1.92 | 1.92 | 1.86 | 1.80 | 1.80 | 1.80 | 1.74 | 1.74 | 1.74 |
| 2.00 | 2.28 | 2.34 | 2.46 | 2.58 | 2.70 | 2.88 | 2.28 | 2.22 | 2.16 | 2.10 | 2.10 | 2.10 | 2.10 | 2.04 | 2.04 | 2.04 | 2.04 | 2.04 |
| 4.00 | 1.38 | 1.74 | 2.58 | 2.70 | 2.22 | 2.22 | 2.22 | 2.22 | 2.22 | 2.22 | 2.22 | 2.22 | 2.22 | 2.22 | 2.22 | 2.22 | 2.22 | 2.22 |
| 6.00 | 1.14 | 1.44 | 1.68 | 1.92 | 2.04 | 2.16 | 2.22 | 2.22 | 2.28 | 2.28 | 2.28 | 2.28 | 2.34 | 2.34 | 2.34 | 2.34 | 2.34 | 2.34 |
| 8.00 | 1.08 | 1.32 | 1.62 | 1.80 | 1.98 | 2.10 | 2.22 | 2.28 | 2.28 | 2.34 | 2.34 | 2.40 | 2.40 | 2.40 | 2.40 | 2.40 | 2.40 | 2.40 |
| 10.00 | 1.02 | 1.32 | 1.56 | 1.74 | 1.92 | 2.04 | 2.16 | 2.28 | 2.34 | 2.34 | 2.40 | 2.40 | 2.46 | 2.46 | 2.46 | 2.46 | 2.46 | 2.46 |
| 12.00 | 1.02 | 1.26 | 1.50 | 1.68 | 1.92 | 2.04 | 2.16 | 2.28 | 2.34 | 2.40 | 2.46 | 2.46 | 2.46 | 2.52 | 2.52 | 2.52 | 2.52 | 2.52 |
| 14.00 | 0.96 | 1.20 | 1.44 | 1.68 | 1.86 | 2.04 | 2.16 | 2.28 | 2.34 | 2.40 | 2.46 | 2.52 | 2.52 | 2.52 | 2.58 | 2.58 | 2.58 | 2.58 |
| 16.00 | 0.96 | 1.20 | 1.44 | 1.68 | 1.86 | 2.04 | 2.16 | 2.28 | 2.40 | 2.46 | 2.46 | 2.52 | 2.52 | 2.58 | 2.58 | 2.58 | 2.58 | 2.64 |
| 18.00 | 0.96 | 1.20 | 1.44 | 1.62 | 1.86 | 2.04 | 2.16 | 2.28 | 2.40 | 2.46 | 2.52 | 2.52 | 2.58 | 2.58 | 2.64 | 2.64 | 2.64 | 2.64 |
| 20.00 | 0.96 | 1.20 | 1.44 | 1.62 | 1.80 | 1.98 | 2.16 | 2.28 | 2.40 | 2.46 | 2.52 | 2.58 | 2.58 | 2.64 | 2.64 | 2.64 | 2.64 | 2.64 |
| 22.00 | 0.96 | 1.20 | 1.38 | 1.62 | 1.80 | 1.98 | 2.16 | 2.28 | 2.40 | 2.46 | 2.52 | 2.58 | 2.64 | 2.64 | 2.64 | 2.70 | 2.70 | 2.70 |
| 24.00 | 0.96 | 1.14 | 1.38 | 1.62 | 1.80 | 1.98 | 2.16 | 2.28 | 2.40 | 2.52 | 2.58 | 2.58 | 2.64 | 2.64 | 2.70 | 2.70 | 2.70 | 2.70 |
| 26.00 | 0.90 | 1.14 | 1.38 | 1.62 | 1.80 | 1.98 | 2.16 | 2.28 | 2.40 | 2.52 | 2.58 | 2.64 | 2.64 | 2.70 | 2.70 | 2.70 | 2.70 | 2.70 |
| 28.00 | 0.90 | 1.14 | 1.38 | 1.62 | 1.80 | 1.98 | 2.16 | 2.28 | 2.40 | 2.52 | 2.58 | 2.64 | 2.64 | 2.70 | 2.70 | 2.70 | 2.70 | 2.76 |
| 30.00 | 0.90 | 1.14 | 1.38 | 1.62 | 1.80 | 1.98 | 2.16 | 2.28 | 2.40 | 2.52 | 2.58 | 2.64 | 2.70 | 2.70 | 2.70 | 2.76 | 2.76 | 2.76 |
| 32.00 | 0.90 | 1.14 | 1.38 | 1.56 | 1.80 | 1.98 | 2.16 | 2.28 | 2.40 | 2.52 | 2.58 | 2.64 | 2.70 | 2.70 | 2.70 | 2.76 | 2.76 | 2.76 |
| 34.00 | 0.90 | 1.14 | 1.38 | 1.56 | 1.80 | 1.98 | 2.16 | 2.28 | 2.40 | 2.52 | 2.58 | 2.64 | 2.70 | 2.70 | 2.76 | 2.76 | 2.76 | 2.76 |
| 36.00 | 0.90 | 1.14 | 1.38 | 1.56 | 1.80 | 1.98 | 2.16 | 2.28 | 2.46 | 2.52 | 2.58 | 2.64 | 2.70 | 2.70 | 2.76 | 2.76 | 2.76 | 2.76 |
| 38.00 | 0.90 | 1.14 | 1.38 | 1.56 | 1.80 | 1.98 | 2.16 | 2.28 | 2.46 | 2.52 | 2.64 | 2.64 | 2.70 | 2.76 | 2.76 | 2.76 | 2.76 | 2.82 |

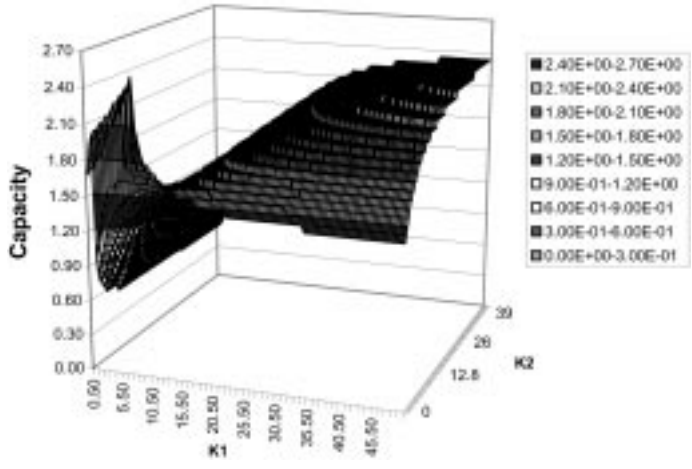


Fig. 4(a) The distribution of the capacities of the follower force at $\bar{K}_3 = 5$

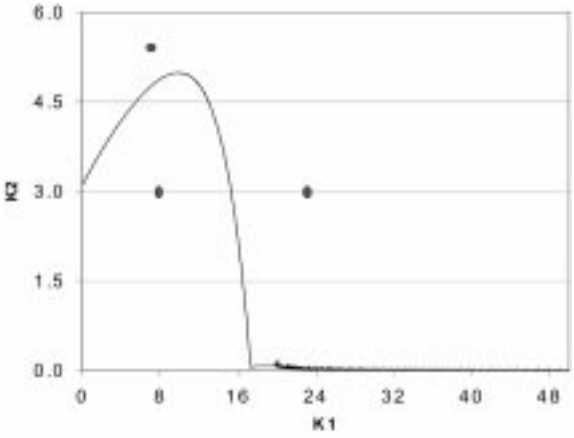


Fig. 4(b) The transition curve of the flutter and buckling instability at $\bar{K}_3 = 5$

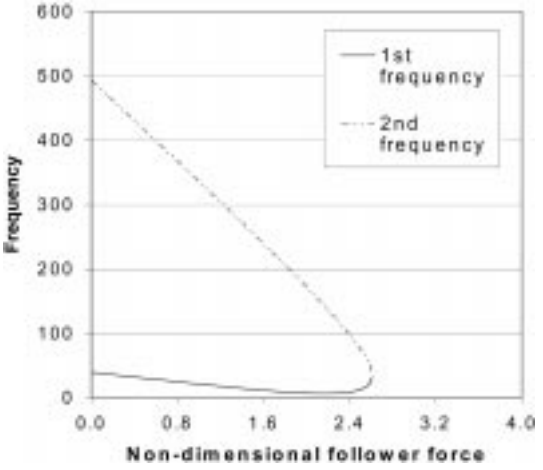


Fig. 4(c) Variation of the first two frequencies at (10,3)

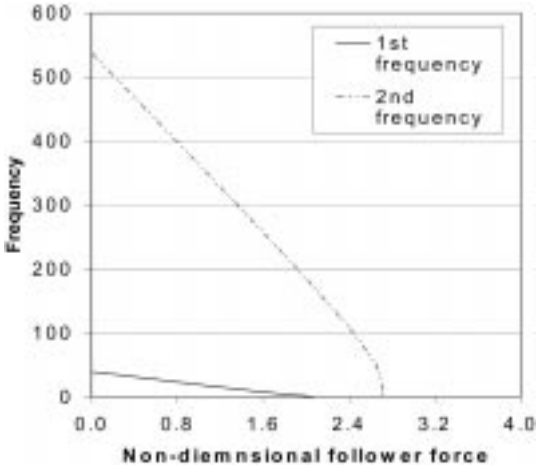


Fig. 4(d) Variation of the first two frequencies at (10,5.5)

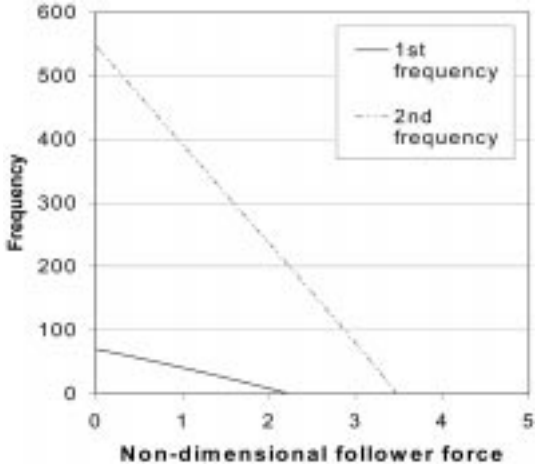


Fig. 4(e) Variation of the first two frequencies at (25,3)

form of flutter, otherwise, the buckling will be the only form of the instability. In accordance with the above statements, in Table 4, the capacities for flutter type of instability are again shaded with grey colour to differentiate them from others for buckling instability. Similarly, the variation of frequencies at three pairs of $\bar{k}_1$-$\bar{k}_2$, i.e. (10,3), (10,5.5), and (25,3) dotted in Fig. 4(b), are shown in Figs. 4(c)-(e). The capacity for flutter is read clearly from Fig. 4(c) as the two frequencies coalesce at $\bar{P} \approx 2.61$. The capacities for buckling are also read from Figs. 4(d)-(e) since in the two figures the first frequencies approach zero at $\bar{P} \approx 2.07$ and $\bar{P} \approx 2.20$ respectively.

### *3.3.4 Capacity of the follower force at $\bar{k}_3 = 10$*

Table 5 lists the capacities of the non-dimensional follower force $\bar{P}$ at $\bar{k}_3 = 10$. From Fig. 5(a) which shows the distribution of the capacities, it shows that the region of the irregularity is enlarged. This phenomenon can also be viewed from Fig. 5(c), in which the transition curve for the different

Table 5 The capacities of the non-dimensional follower force $\bar{P}$ at $\bar{K}_3 = 10$

| $\bar{k}_2$ \ $\bar{k}_1$ | 2.50 | 5.00 | 7.50 | 10.00 | 12.50 | 15.00 | 17.50 | 20.00 | 22.50 | 25.00 | 27.50 | 30.00 | 32.50 | 35.00 | 37.50 | 40.00 | 42.50 | 45.00 |
|---|---|---|---|---|---|---|---|---|---|---|---|---|---|---|---|---|---|---|
| 0.00 | 1.92 | 2.04 | 2.16 | 2.34 | 2.52 | 2.70 | 2.88 | 3.06 | 3.24 | 2.58 | 2.40 | 2.28 | 2.22 | 2.16 | 2.10 | 2.10 | 2.04 | 2.04 |
| 2.00 | 2.40 | 2.46 | 2.52 | 2.64 | 2.76 | 2.82 | 2.94 | 3.06 | 3.24 | 2.64 | 2.58 | 2.52 | 2.46 | 2.40 | 2.40 | 2.40 | 2.34 | 2.34 |
| 4.00 | 2.58 | 2.64 | 2.70 | 2.76 | 2.88 | 2.94 | 3.00 | 3.12 | 3.24 | 2.70 | 2.64 | 2.64 | 2.58 | 2.58 | 2.58 | 2.58 | 2.58 | 2.52 |
| 6.00 | 1.38 | 1.74 | 2.10 | 2.88 | 2.94 | 3.00 | 3.06 | 3.12 | 2.82 | 2.76 | 2.70 | 2.70 | 2.70 | 2.70 | 2.70 | 2.70 | 2.70 | 2.70 |
| 8.00 | 1.26 | 1.56 | 1.86 | 2.10 | 2.34 | 2.52 | 2.70 | 2.76 | 2.76 | 2.76 | 2.76 | 2.76 | 2.76 | 2.76 | 2.76 | 2.76 | 2.76 | 2.76 |
| 10.00 | 1.20 | 1.50 | 1.74 | 1.98 | 2.22 | 2.40 | 2.52 | 2.64 | 2.76 | 2.76 | 2.82 | 2.82 | 2.82 | 2.82 | 2.82 | 2.82 | 2.82 | 2.82 |
| 12.00 | 1.14 | 1.44 | 1.68 | 1.92 | 2.10 | 2.34 | 2.46 | 2.64 | 2.70 | 2.76 | 2.82 | 2.82 | 2.88 | 2.88 | 2.88 | 2.88 | 2.88 | 2.88 |
| 14.00 | 1.14 | 1.38 | 1.62 | 1.86 | 2.10 | 2.28 | 2.46 | 2.58 | 2.70 | 2.76 | 2.82 | 2.88 | 2.88 | 2.88 | 2.94 | 2.94 | 2.94 | 2.94 |
| 16.00 | 1.14 | 1.38 | 1.62 | 1.86 | 2.04 | 2.22 | 2.40 | 2.58 | 2.70 | 2.82 | 2.88 | 2.88 | 2.94 | 2.94 | 2.94 | 2.94 | 2.94 | 3.00 |
| 18.00 | 1.08 | 1.32 | 1.56 | 1.80 | 2.04 | 2.22 | 2.40 | 2.58 | 2.70 | 2.82 | 2.88 | 2.94 | 2.94 | 2.94 | 3.00 | 3.00 | 3.00 | 3.00 |
| 20.00 | 1.08 | 1.32 | 1.56 | 1.80 | 1.98 | 2.22 | 2.40 | 2.58 | 2.70 | 2.82 | 2.88 | 2.94 | 2.94 | 3.00 | 3.00 | 3.00 | 3.00 | 3.06 |
| 22.00 | 1.08 | 1.32 | 1.56 | 1.80 | 1.98 | 2.16 | 2.40 | 2.52 | 2.70 | 2.82 | 2.88 | 2.94 | 3.00 | 3.00 | 3.00 | 3.06 | 3.06 | 3.06 |
| 24.00 | 1.08 | 1.32 | 1.56 | 1.74 | 1.98 | 2.16 | 2.34 | 2.52 | 2.70 | 2.82 | 2.88 | 2.94 | 3.00 | 3.00 | 3.06 | 3.06 | 3.06 | 3.06 |
| 26.00 | 1.08 | 1.32 | 1.56 | 1.74 | 1.98 | 2.16 | 2.34 | 2.52 | 2.70 | 2.82 | 2.88 | 3.00 | 3.00 | 3.06 | 3.06 | 3.06 | 3.06 | 3.12 |
| 28.00 | 1.08 | 1.32 | 1.50 | 1.74 | 1.98 | 2.16 | 2.34 | 2.52 | 2.70 | 2.82 | 2.94 | 3.00 | 3.00 | 3.06 | 3.06 | 3.06 | 3.12 | 3.12 |
| 30.00 | 1.08 | 1.26 | 1.50 | 1.74 | 1.92 | 2.16 | 2.34 | 2.52 | 2.70 | 2.82 | 2.94 | 3.00 | 3.06 | 3.06 | 3.06 | 3.12 | 3.12 | 3.12 |
| 32.00 | 1.02 | 1.26 | 1.50 | 1.74 | 1.92 | 2.16 | 2.34 | 2.52 | 2.70 | 2.82 | 2.94 | 3.00 | 3.06 | 3.06 | 3.12 | 3.12 | 3.12 | 3.12 |
| 34.00 | 1.02 | 1.26 | 1.50 | 1.74 | 1.92 | 2.16 | 2.34 | 2.52 | 2.70 | 2.82 | 2.94 | 3.00 | 3.06 | 3.12 | 3.12 | 3.12 | 3.12 | 3.12 |
| 36.00 | 1.02 | 1.26 | 1.50 | 1.74 | 1.92 | 2.16 | 2.34 | 2.52 | 2.70 | 2.82 | 2.94 | 3.00 | 3.06 | 3.12 | 3.12 | 3.12 | 3.12 | 3.18 |
| 38.00 | 1.02 | 1.26 | 1.50 | 1.74 | 1.92 | 2.10 | 2.34 | 2.52 | 2.70 | 2.82 | 2.94 | 3.00 | 3.06 | 3.12 | 3.12 | 3.12 | 3.18 | 3.18 |

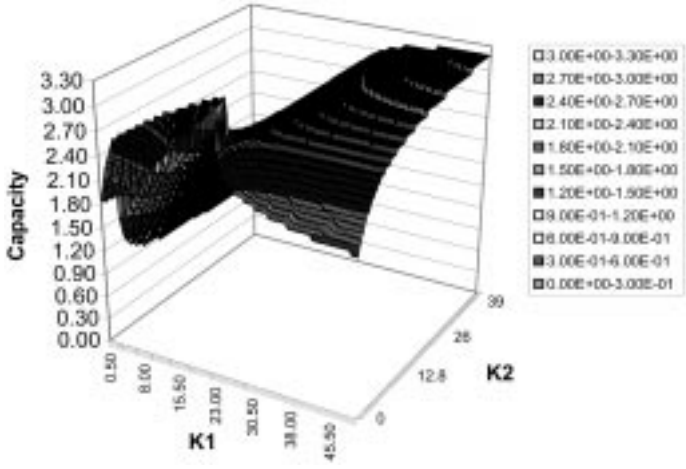


Fig. 5(a) The distribution of the capacities of the follower force at $\bar{K}_3 = 10$

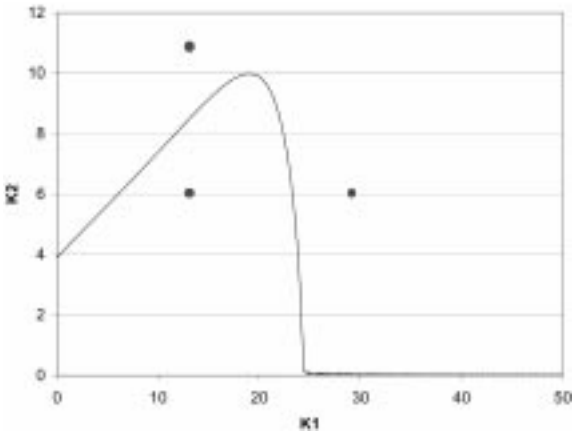


Fig. 5(b) The boundary line of the flutter and buckling instability at $\bar{K}_3 = 10$

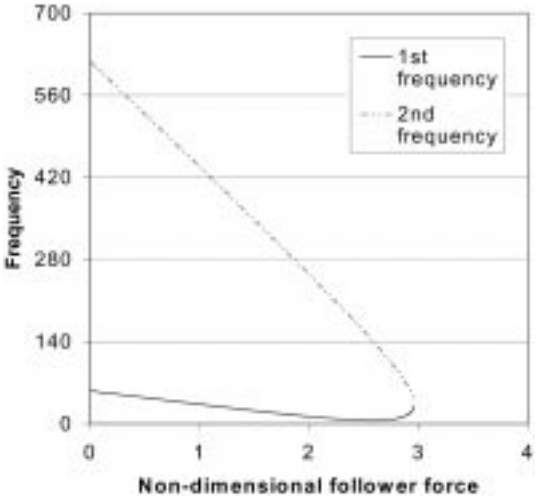


Fig. 5(c) Variation of the first two frequencies at (15,6)

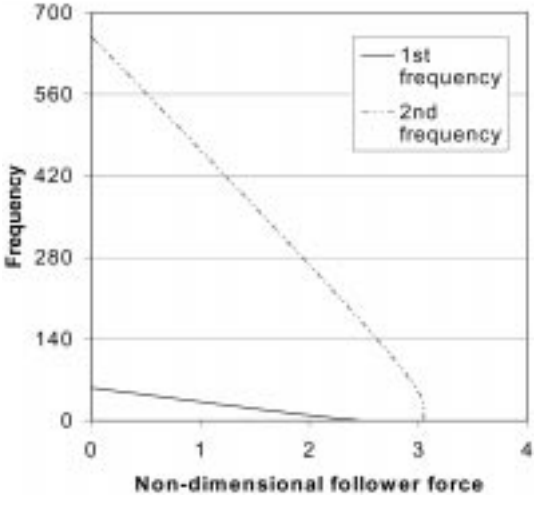


Fig. 5(d) Variation of the first two frequencies at (15,11)

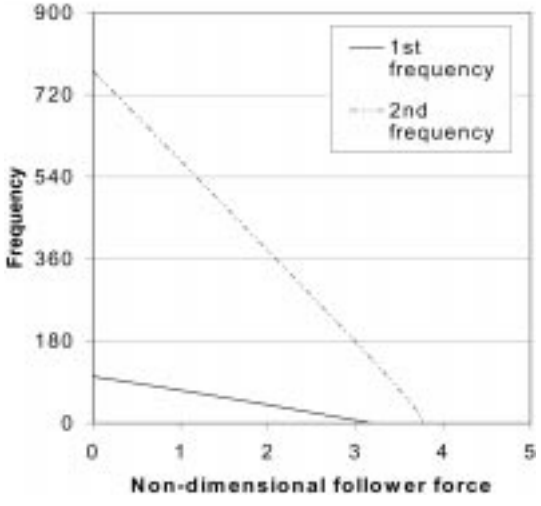


Fig. 5(e) Variation of the first two frequencies at (30,6)

forms of the instability is drawn. The enlarged region for flutter is also reflected from the shaded portion in Table 5. The pair of $\bar{k}_1$-$\bar{k}_2$ at (15, 6) is under the curve indicating that the instability at this point is in the form of flutter. The variation of the frequencies at this point is shown in Fig. 5(c), in which the flutter capacity is read as $\bar{P} \approx 3.00$. The other two pairs at (15,11) and (30,6) are outside the curve, and hence the buckling capacities can be read from Fig. 5(d)-(e) as $\bar{P} \approx 2.44$ and $\bar{P} \approx 2.70$.

### *3.3.5 Capacity of the follower force at $\bar{k}_3 = 20$*

Again, the capacities of the follower force for flutter buckling of the beam is listed in Table 6 and their distribution is plotted in Fig. 6(a). Similar observation is obtained that the shaded portion in Table 6 is enlarged as well. The transition curve to differentiate the forms of instability is shown in

Table 6 The capacities of the non-dimensional follower force $\bar{P}$ at $\bar{K}_3 = 20$

| $\bar{k}_2$ \ $\bar{k}_1$ | 2.50 | 5.00 | 7.50 | 10.00 | 12.50 | 15.00 | 17.50 | 20.00 | 22.50 | 25.00 | 27.50 | 30.00 | 32.50 | 35.00 | 37.50 | 40.00 | 42.50 | 45.00 |
|---|---|---|---|---|---|---|---|---|---|---|---|---|---|---|---|---|---|---|
| 0.00 | 1.98 | 2.10 | 2.22 | 2.34 | 2.52 | 2.70 | 2.82 | 3.00 | 3.18 | 3.30 | 3.48 | 2.76 | 2.58 | 2.52 | 2.40 | 2.34 | 2.34 | 2.28 |
| 2.00 | 2.52 | 2.58 | 2.64 | 2.70 | 2.82 | 2.94 | 3.00 | 3.12 | 3.24 | 3.36 | 3.48 | 2.94 | 2.82 | 2.76 | 2.70 | 2.64 | 2.64 | 2.64 |
| 4.00 | 2.76 | 2.76 | 2.82 | 2.88 | 2.94 | 3.06 | 3.12 | 3.18 | 3.30 | 3.36 | 3.48 | 3.06 | 2.94 | 2.88 | 2.88 | 2.82 | 2.82 | 2.82 |
| 6.00 | 1.56 | 1.98 | 2.94 | 3.00 | 3.06 | 3.12 | 3.18 | 3.24 | 3.30 | 3.36 | 3.48 | 3.12 | 3.06 | 3.00 | 3.00 | 2.94 | 2.94 | 2.94 |
| 8.00 | 1.38 | 1.68 | 1.98 | 2.28 | 3.12 | 3.18 | 3.24 | 3.30 | 3.36 | 3.42 | 3.48 | 3.12 | 3.12 | 3.06 | 3.06 | 3.06 | 3.06 | 3.06 |
| 10.00 | 1.32 | 1.62 | 1.86 | 2.10 | 2.34 | 2.64 | 3.24 | 3.30 | 3.36 | 3.42 | 3.48 | 3.18 | 3.12 | 3.12 | 3.12 | 3.12 | 3.12 | 3.12 |
| 12.00 | 1.26 | 1.56 | 1.80 | 2.04 | 2.28 | 2.46 | 2.70 | 2.88 | 3.36 | 3.42 | 3.18 | 3.18 | 3.18 | 3.18 | 3.18 | 3.18 | 3.18 | 3.18 |
| 14.00 | 1.26 | 1.50 | 1.74 | 1.98 | 2.22 | 2.40 | 2.64 | 2.82 | 3.00 | 3.12 | 3.18 | 3.18 | 3.18 | 3.18 | 3.18 | 3.18 | 3.18 | 3.18 |
| 16.00 | 1.20 | 1.44 | 1.68 | 1.92 | 2.16 | 2.34 | 2.58 | 2.76 | 2.94 | 3.06 | 3.18 | 3.18 | 3.24 | 3.24 | 3.24 | 3.24 | 3.24 | 3.24 |
| 18.00 | 1.20 | 1.44 | 1.68 | 1.92 | 2.10 | 2.34 | 2.52 | 2.70 | 2.88 | 3.06 | 3.12 | 3.18 | 3.24 | 3.24 | 3.24 | 3.30 | 3.30 | 3.30 |
| 20.00 | 1.20 | 1.44 | 1.68 | 1.86 | 2.10 | 2.28 | 2.52 | 2.70 | 2.88 | 3.00 | 3.12 | 3.24 | 3.24 | 3.30 | 3.30 | 3.30 | 3.30 | 3.30 |
| 22.00 | 1.14 | 1.44 | 1.62 | 1.86 | 2.10 | 2.28 | 2.46 | 2.70 | 2.82 | 3.00 | 3.12 | 3.24 | 3.24 | 3.30 | 3.30 | 3.30 | 3.30 | 3.30 |
| 24.00 | 1.14 | 1.38 | 1.62 | 1.86 | 2.04 | 2.28 | 2.46 | 2.64 | 2.82 | 3.00 | 3.12 | 3.24 | 3.30 | 3.30 | 3.30 | 3.36 | 3.36 | 3.36 |
| 26.00 | 1.14 | 1.38 | 1.62 | 1.86 | 2.04 | 2.28 | 2.46 | 2.64 | 2.82 | 3.00 | 3.12 | 3.24 | 3.30 | 3.30 | 3.36 | 3.36 | 3.36 | 3.36 |
| 28.00 | 1.14 | 1.38 | 1.62 | 1.80 | 2.04 | 2.22 | 2.46 | 2.64 | 2.82 | 3.00 | 3.12 | 3.24 | 3.30 | 3.36 | 3.36 | 3.36 | 3.36 | 3.36 |
| 30.00 | 1.14 | 1.38 | 1.62 | 1.80 | 2.04 | 2.22 | 2.46 | 2.64 | 2.82 | 2.94 | 3.12 | 3.24 | 3.30 | 3.36 | 3.36 | 3.36 | 3.42 | 3.42 |
| 32.00 | 1.14 | 1.38 | 1.62 | 1.80 | 2.04 | 2.22 | 2.40 | 2.64 | 2.82 | 2.94 | 3.12 | 3.24 | 3.30 | 3.36 | 3.36 | 3.42 | 3.42 | 3.42 |
| 34.00 | 1.14 | 1.38 | 1.56 | 1.80 | 2.04 | 2.22 | 2.40 | 2.58 | 2.82 | 2.94 | 3.12 | 3.24 | 3.30 | 3.36 | 3.42 | 3.42 | 3.42 | 3.42 |
| 36.00 | 1.14 | 1.38 | 1.56 | 1.80 | 1.98 | 2.22 | 2.40 | 2.58 | 2.76 | 2.94 | 3.12 | 3.24 | 3.30 | 3.36 | 3.42 | 3.42 | 3.42 | 3.42 |
| 38.00 | 1.14 | 1.38 | 1.56 | 1.80 | 1.98 | 2.22 | 2.40 | 2.58 | 2.76 | 2.94 | 3.12 | 3.24 | 3.36 | 3.36 | 3.42 | 3.42 | 3.42 | 3.42 |

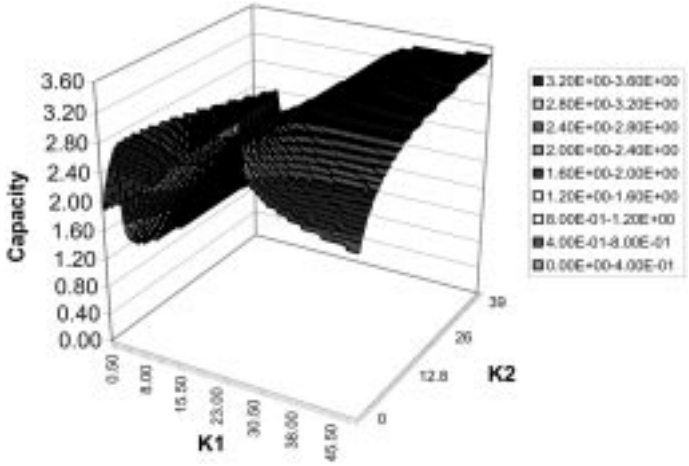


Fig. 6(a) The distribution of the capacities of the follower force at $\bar{K}_3 = 20$

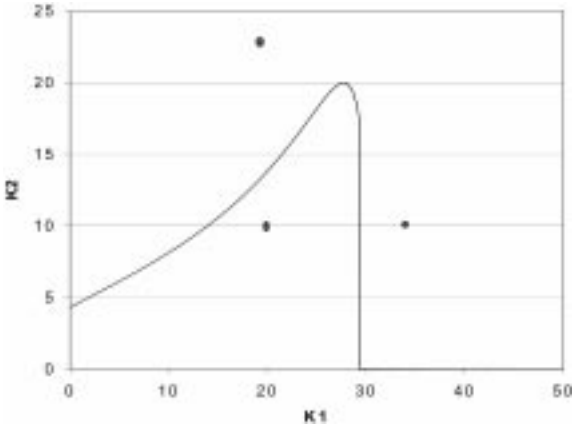


Fig. 6(b) The boundary line of the flutter and buckling instability at $\bar{K}_3 = 20$

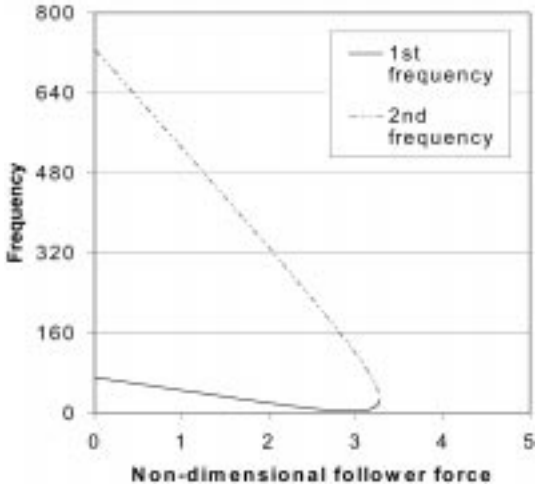


Fig. 6(c) Variation of the first two frequencies at (20,10)

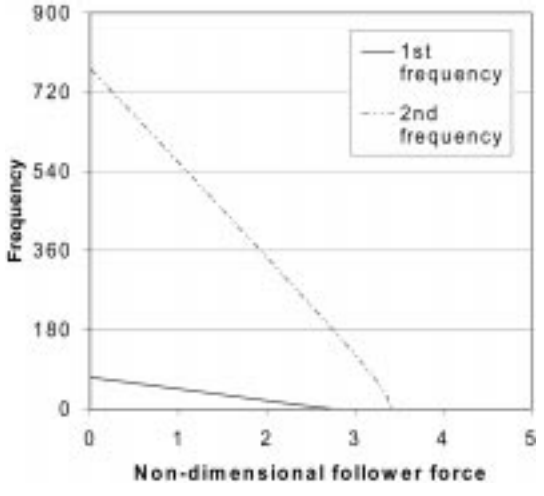


Fig. 6(d) Variation of the first two frequencies at (20,23)

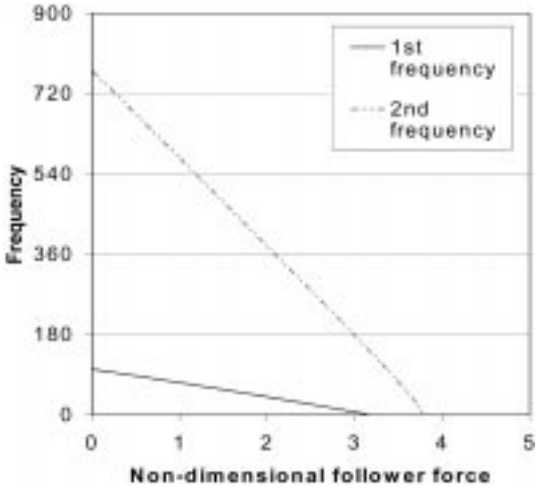


Fig. 6(e) Variation of the first two frequencies at (35,10)

Fig. 6(b). Omitting the repeated descriptions for the Figs. 6(c)-(e), we just list the capacities of the follower force at the pairs of $\bar{k}_1$-$\bar{k}_2$ at (20,10), (20,23), and (35,10) as $\bar{P} \approx 3.30$ for flutter capacity, $\bar{P} \approx 2.70$ and $\bar{P} \approx 3.12$ for buckling capacities respectively.

### *3.3.6 Capacity of the follower force at $\bar{k}_3 = 40$*

The transition curve is plotted in Fig. 7(b). From the comparison of this figure with Fig. 1(c) for the transition curve at $\bar{k}_3 = \infty$, it shows that the results at $\bar{k}_3 = 40$ can be viewed as the asymptotic ones for very large values of $\bar{k}_3$. The capacities of the follower force for the instability

Table 7 The capacities of the non-dimensional follower force $\overline{P}$ at $\overline{K}_3 = 40$

| $\overline{k}_2$ \ $\overline{k}_1$ | 2.50 | 5.00 | 7.50 | 10.00 | 12.50 | 15.00 | 17.50 | 20.00 | 22.50 | 25.00 | 27.50 | 30.00 | 32.50 | 35.00 | 37.50 | 40.00 | 42.50 | 45.00 |
|---|---|---|---|---|---|---|---|---|---|---|---|---|---|---|---|---|---|---|
| 0.00 | 2.04 | 2.16 | 2.28 | 2.40 | 2.58 | 2.70 | 2.88 | 3.00 | 3.18 | 3.36 | 3.48 | 3.60 | 2.94 | 2.76 | 2.64 | 2.58 | 2.52 | 2.46 |
| 2.00 | 2.58 | 2.64 | 2.70 | 2.82 | 2.88 | 3.00 | 3.06 | 3.18 | 3.30 | 3.36 | 3.48 | 3.60 | 3.12 | 3.00 | 2.88 | 2.82 | 2.82 | 2.76 |
| 4.00 | 2.82 | 2.88 | 2.94 | 3.00 | 3.06 | 3.12 | 3.18 | 3.24 | 3.36 | 3.42 | 3.54 | 3.60 | 3.24 | 3.12 | 3.06 | 3.00 | 3.00 | 2.94 |
| 6.00 | 1.68 | 2.10 | 3.06 | 3.12 | 3.12 | 3.18 | 3.24 | 3.30 | 3.36 | 3.48 | 3.54 | 3.60 | 3.30 | 3.24 | 3.18 | 3.12 | 3.12 | 3.12 |
| 8.00 | 1.44 | 1.80 | 2.10 | 2.40 | 3.24 | 3.24 | 3.30 | 3.36 | 3.42 | 3.48 | 3.54 | 3.60 | 3.36 | 3.30 | 3.24 | 3.24 | 3.18 | 3.18 |
| 10.00 | 1.38 | 1.68 | 1.92 | 2.22 | 2.46 | 2.70 | 3.36 | 3.42 | 3.42 | 3.48 | 3.54 | 3.66 | 3.42 | 3.30 | 3.30 | 3.30 | 3.30 | 3.24 |
| 12.00 | 1.32 | 1.62 | 1.86 | 2.10 | 2.34 | 2.58 | 2.76 | 3.42 | 3.48 | 3.54 | 3.60 | 3.66 | 3.42 | 3.36 | 3.36 | 3.36 | 3.36 | 3.30 |
| 14.00 | 1.32 | 1.56 | 1.80 | 2.04 | 2.28 | 2.46 | 2.70 | 2.88 | 3.12 | 3.54 | 3.60 | 3.66 | 3.42 | 3.42 | 3.36 | 3.36 | 3.36 | 3.36 |
| 16.00 | 1.26 | 1.50 | 1.74 | 1.98 | 2.22 | 2.40 | 2.64 | 2.82 | 3.00 | 3.18 | 3.60 | 3.66 | 3.42 | 3.42 | 3.42 | 3.42 | 3.42 | 3.42 |
| 18.00 | 1.26 | 1.50 | 1.74 | 1.98 | 2.16 | 2.40 | 2.58 | 2.76 | 2.94 | 3.12 | 3.30 | 3.42 | 3.42 | 3.42 | 3.42 | 3.42 | 3.42 | 3.42 |
| 20.00 | 1.26 | 1.50 | 1.68 | 1.92 | 2.16 | 2.34 | 2.58 | 2.76 | 2.94 | 3.12 | 3.24 | 3.36 | 3.42 | 3.48 | 3.48 | 3.48 | 3.48 | 3.48 |
| 22.00 | 1.20 | 1.44 | 1.68 | 1.92 | 2.10 | 2.34 | 2.52 | 2.70 | 2.88 | 3.06 | 3.24 | 3.36 | 3.42 | 3.48 | 3.48 | 3.48 | 3.48 | 3.48 |
| 24.00 | 1.20 | 1.44 | 1.68 | 1.92 | 2.10 | 2.34 | 2.52 | 2.70 | 2.88 | 3.06 | 3.24 | 3.36 | 3.42 | 3.48 | 3.48 | 3.48 | 3.54 | 3.54 |
| 26.00 | 1.20 | 1.44 | 1.68 | 1.86 | 2.10 | 2.28 | 2.52 | 2.70 | 2.88 | 3.06 | 3.24 | 3.36 | 3.42 | 3.48 | 3.54 | 3.54 | 3.54 | 3.54 |
| 28.00 | 1.20 | 1.44 | 1.68 | 1.86 | 2.10 | 2.28 | 2.46 | 2.70 | 2.88 | 3.06 | 3.18 | 3.36 | 3.42 | 3.48 | 3.54 | 3.54 | 3.54 | 3.54 |
| 30.00 | 1.20 | 1.44 | 1.62 | 1.86 | 2.10 | 2.28 | 2.46 | 2.64 | 2.88 | 3.00 | 3.18 | 3.36 | 3.48 | 3.54 | 3.54 | 3.54 | 3.54 | 3.54 |
| 32.00 | 1.20 | 1.44 | 1.62 | 1.86 | 2.04 | 2.28 | 2.46 | 2.64 | 2.82 | 3.00 | 3.18 | 3.36 | 3.48 | 3.54 | 3.54 | 3.54 | 3.60 | 3.60 |
| 34.00 | 1.20 | 1.38 | 1.62 | 1.86 | 2.04 | 2.28 | 2.46 | 2.64 | 2.82 | 3.00 | 3.18 | 3.36 | 3.48 | 3.54 | 3.54 | 3.60 | 3.60 | 3.60 |
| 36.00 | 1.20 | 1.38 | 1.62 | 1.86 | 2.04 | 2.28 | 2.46 | 2.64 | 2.82 | 3.00 | 3.18 | 3.30 | 3.48 | 3.54 | 3.60 | 3.60 | 3.60 | 3.60 |
| 38.00 | 1.20 | 1.38 | 1.62 | 1.86 | 2.04 | 2.22 | 2.46 | 2.64 | 2.82 | 3.00 | 3.18 | 3.30 | 3.48 | 3.54 | 3.60 | 3.60 | 3.60 | 3.60 |

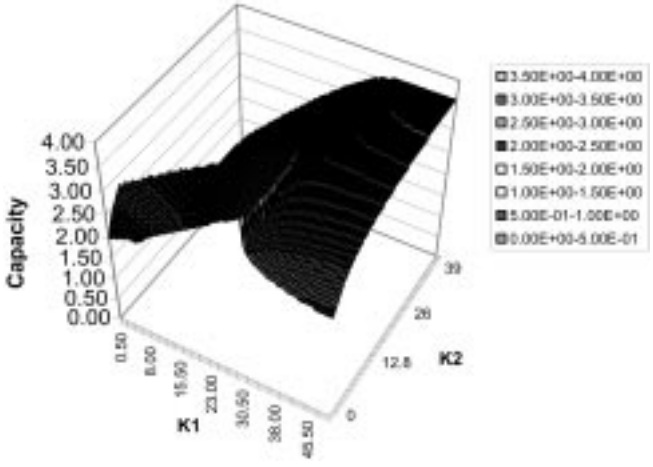


Fig. 7(a) The distribution of the capacities of the follower force at $\overline{K}_3 = 40$

of the beam and their distribution are shown in Table 7 and Fig. 7(a). From the top view of Fig. 7(a), some observations are investigated as follows. For the domain of the co-existence of the two instability forms when $\overline{k}_1 < 34.8$, the capacities for flutter increase with the increase of $\overline{k}_2$. Then there is an abrupt decrease for the capacity around the transition point from flutter to buckling. For example at $\overline{k}_1$-$\overline{k}_2$ of (0, 4.6), Fig. 7(a) shows an abrupt drop of the capacity. After this transition

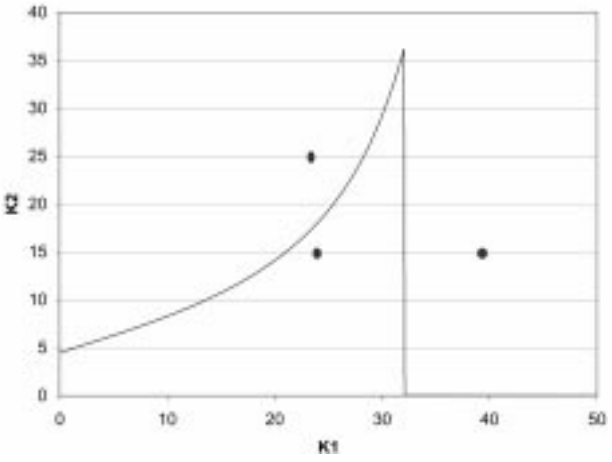


Fig. 7(b) The boundary line of the flutter and buckling instability at $\overline{K}_3 = 20$

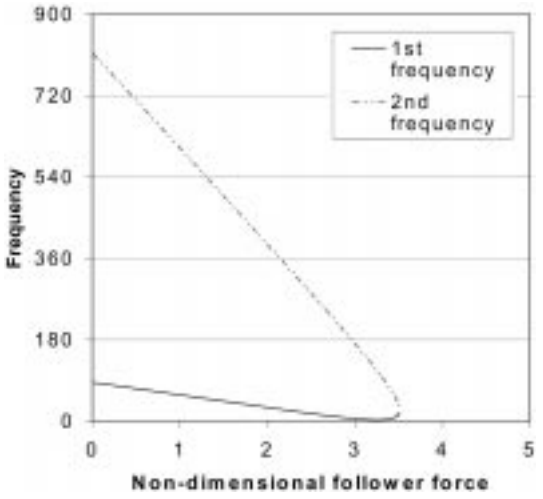


Fig. 7(c) Variation of the first two frequencies at (25,15)

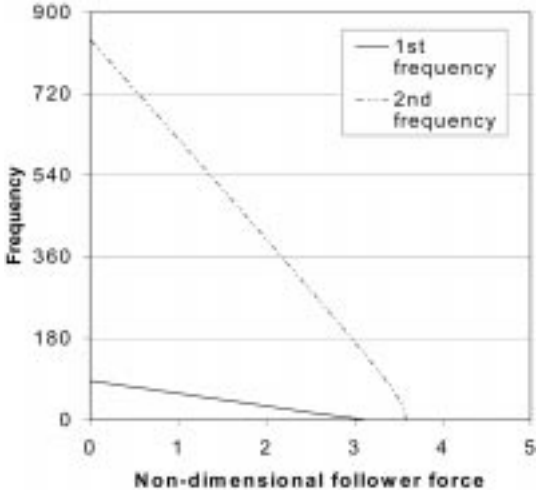


Fig. 7(d) Variation of the first two frequencies at (25,25)

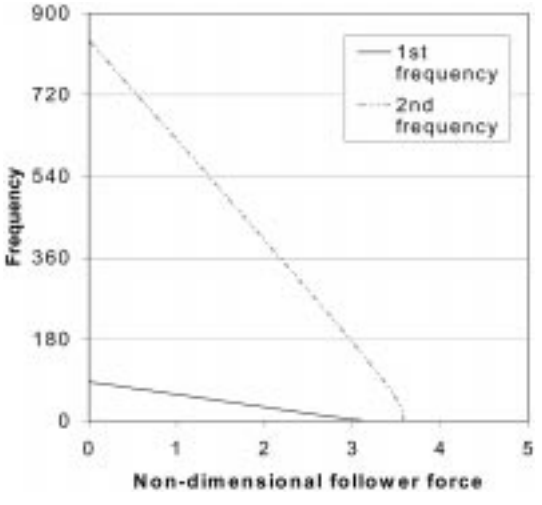


Fig. 7(e) Variation of the first two frequencies at (40,15)

point, the buckling capacities decrease smoothly and finally come to the asymptotic solution. Things become different after the co-existence region of the two instability regions. When $\overline{k}_1 > 34.8$, only buckling governs the instability form. The capacities increase smoothly with increase of $\overline{k}_2$, and finally come to asymptotic results. Similar observations are also found in Figs. 3(a)-6(a) for the distributions of the capacities of follower force. Three pairs of $\overline{k}_1$-$\overline{k}_2$ at (25,15), (25,25), and (40,15) are dotted in Figs. 7(c)-(e). The flutter capacity for the follower force at (25,15) is read as $\overline{P} \approx 3.54$, and the buckling capacities at (25,25) and (40,15) are $\overline{P} \approx 3.08$ and $\overline{P} \approx 3.40$.

## 4. Conclusions

The paper studies the flutter and buckling analysis of a general beam structure subjected to a static follower force. The analytical solutions for the flutter and buckling capacities versus the different spring stiffness are obtained. The transition surface for the differentiation of flutter and buckling of the beam is obtained with respect to the stiffness of the springs. The capacities of the follower force for the flutter and buckling of the beam are obtained by studying the variations of the first two frequencies of the beam structure. The phenomena of the abrupt change in the capacity distributions are found to be the indicators of the boundary of flutter and buckling of the beam.

This research may be used as a benchmark for the flutter and buckling analysis of beams. The phenomenon of co-existence of flutter and buckling in the general beam structure is important in the stability analysis of structures. The potential of the research is in the stability design and control of the structures.

## Acknowledgements

The author appreciates the constructive comments from the reviewers.

## References

Alfutov, N.A. (1999), *Stability of Elastic Structures*. Springer-Verlag, Berlin.

Anderson, S.B. and Thompsen, J.J. (2002), "Post-critical behaviour of Beck's column with a tip mass", *Int. J. Non-linear Mech.*, **37**, 131-151.

Atanackvic, T.M. and Cveticanin, L. (1994), "Dynamics of in-plane motion of a robot arm. in Mechatronics", 147-152. Acar, M.J. Makra and E. Penny editors. Computational Mech. Publ. Boston.

Bailey, C. and Haines, J.L. (1981), "Vibration and stability of non-conservative follower force systems", *Comput. Meth. Appl. Mech. Eng.*, **26**, 1-31.

Beck, M. (1952), "Die Knicklast des einseitig eingespannten tangential gedruckten Stabes", *Z. Angew. Math. Phys*., **3**.

Bolotin, V.V. (1963), *Non-conservative Problems of the Theory of Elastic Stability.* Macmillan, New York.

Bolotin, V.V., Grishko, A.A., Kounadis, A.N. and Gants, C.J. (1998), "Non-linear panel flutter in remote post-critical domains", *Int. J. Non-linear Mech.*, **33**, 753-764.

Carr, J. and Malhardeen, M.Z.M. (1979), " Beck's problem", *SIAM Journal of Applied Mathematics*, **37**, 261-262.

Deineko, K.S. and Leonov, M.IA. (1955), *The Dynamic Method of Investigating the Stability of a Bar in Compression.* PMM. 19.

Feodos'ev, V.I. (1953), *Selected Problems and Questions in Strength of Materials*. Gostekhizdat.

Hauger, W. and Vetter, K. (1976), "Influence of an elastic foundation on the stability of a tangentially loaded column", *J. Sound Vib.*, **47**, 296-299.

Hanaoka, M. and Washizu, K. (1979), "Optimum design of Beck's column", *Comput. Struct.*, **11**, 473-480.

Jankovic, M.S. (1993), "Comments on 'Eigenvalue sensitivity in the stability analysis of Beck's column with a concentrated Mass at the free end", *J. Sound Vib.*, **167**, 557-559.

Kounadis, A.N. (1981), "Divergence and flutter instability of elastically restrained structures under follower forces", *Int. J. Eng. Sci.*, **19**, 553-562.

Kounadis, A.N. (1983), "The existence of regions of divergence instability for nonconservative systems under follower forces", *Int. J. Solids Struct.*, **19**, 725-733.

Kounadis, A.N. (1991), "Some new instability aspects for nonconservative systems under follower loads", *Int. J.*

*Mech. Sci.*, **33**, 297-311.
Kounadis, A.N. and Katsikadelis (1980), "On the discontinuity of the flutter load for various types of cantilevers", *Int. J. Solids Struct.*, **16**, 375-383.
Kounadis, A.N. (1998), "Qualitative criteria for dynamic buckling of imperfection sensitive nonconservative systems", *Int. J. Mech. Sci.*, **40**, 949-962.
Langthjem, M.A. and Sugiyama, Y. (2000), "Optimum design of cantilevered columns under the combined action of conservative and nonconservation loads: Part I: The undamped case", *Comput. Struct.*, **74**, 385-398.
Leipholz, H. (1983), "Assessing stability of elastic systems by considering their small Vibrations", *Ingenieur-Archiv.*, **53**, 345-362.
Matsuda, H., Sakiyama, T. and Morita, Ch. (1993), "Variable cross sectional Beck's column subjected to non-conservative load", *Zeitschrift fur angwandte Mathematik und Mechanik* (ZAMM), **73**, 383-385.
Pedersen, Pauli. (1977), " Influence of boundary conditions on the stability of a column under non-conservative load", *Int. J. Solids Struct.*, **13**, 445-455.
Pfluger, A. (1950), *Stabilitats Probleme Der Elastostatik*, Springer-Verlag, Berlin.
Ryu, Si-Ung and Sugiyama, Y. (2003), "Computational dynamics approach to the effect of damping on stability of a cantilevered column subjected to a follower force", *Comput. Struct.*, **81**, 265-271.
Sugiyama, Y., Katayama, K. and Kinoi, S. (1995), "Flutter of cantilevered column under rocket thrust", *J. Aerospace Eng.*, **8**, 9-15.
Sundararajan, C. (1974), "Stability of columns on elastic foundations subjected to conservative and non-conservative forces", *J. Sounds Vib.*, **37**, 79-85.
Timoshenko, S.P. and Gere, J.M. (1961), *Theory of Elastic Stability.* McGraw-Hill International Book Company, Singapore.
Wang, Q. and Quek, S.T. (2002), "Enhancing flutter and buckling capacity of column by piezoelectric layers", *Int. J. Solids Struct.*, **39**, 4167-4180.